Research Based Science Education

2000

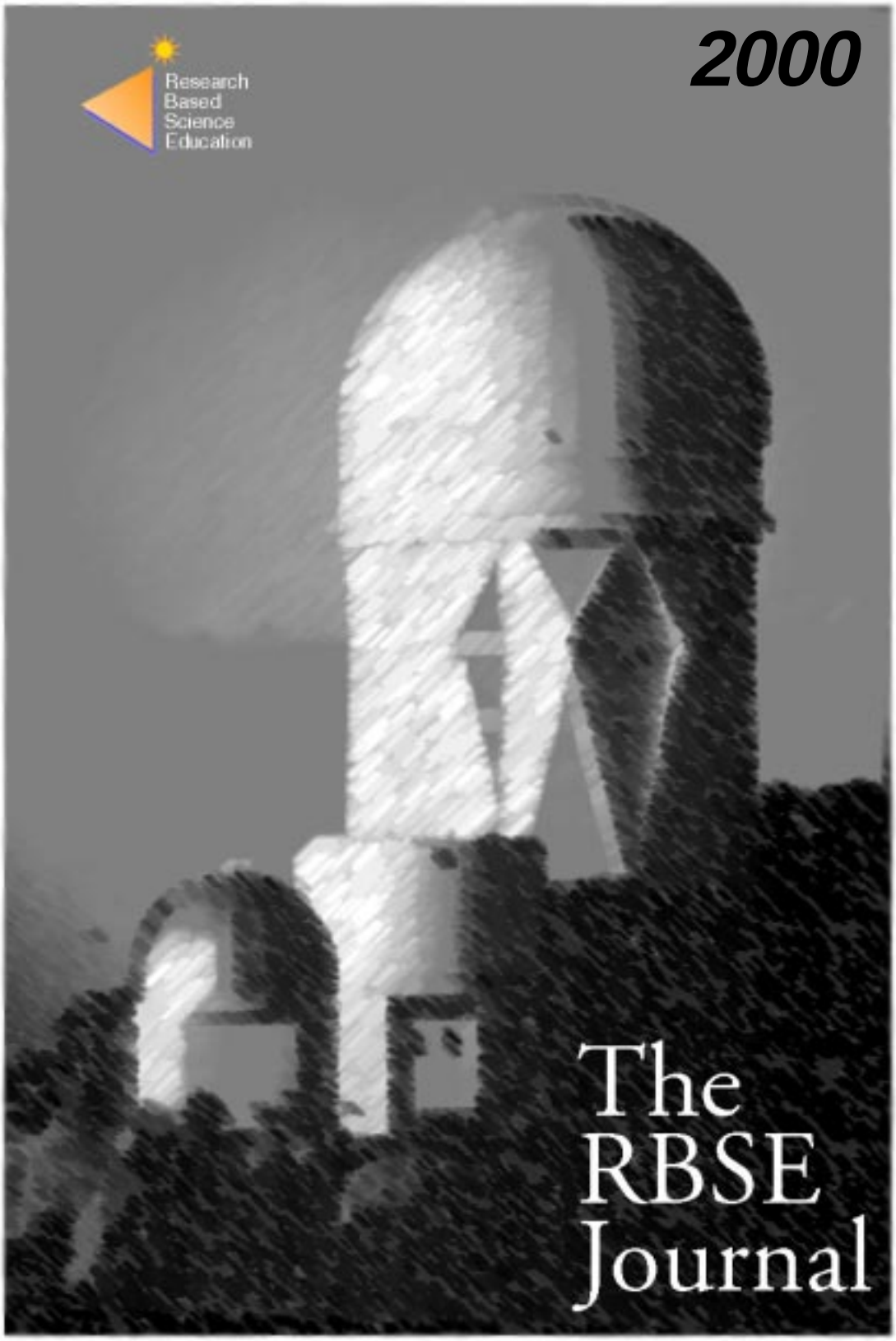

The RBSE Journal

AURA

National Optical Astronomy Observatory

NSF

The RBSE Journal

2000

The "Use of Astronomy in Research Based Science Education" (RBSE) is a Teacher Enhancement Program funded by the National Science Foundation. It consists of a four-week summer workshop for middle and high school teachers interested in incorporating astronomy research within their science classes. RBSE extends the experience to the classroom with materials, datasets, support and mentors during the academic year. The RBSE Journal is an annual publication intended to present the research of students participating in the RBSE program.

Table of Contents

Solar Research:

4 **Sunspots and Earthquakes**
José Santiago
Sabana Llana Middle School, Río Piedras, Puerto Rico
Teacher: Maria Hernández, RBSE '99

6 **Sunspots and Hurricanes**
Carlos F. Ramírez
Sabana Llana Middle School, Río Piedras, Puerto Rico
Teacher: Maria Hernández, RBSE '99

8 **Identifying Unknown Solar Absorption Lines**
Todd Faner and Regan Wilson
Grosse Pointe North High School, Grosse Point, MI
Teacher: Ardis Maciolek, RBSE '98

12 **The Effect of Sunspots on Temperature and Ultraviolet Rays**
Jessy Farrell, Heather McPherson, and Yasmin Afsar
Chenery Middle School, Belmont MA
Teacher: Elizabeth Chait-Sanghavi, RBSE '98

16 **Sunspots and Flight Safety**
Kirby Tyrrell, Catherine Caruso and Emilie Anderson
Chenery Middle School, Belmont MA
Teacher: Elizabeth Chait-Sanghavi, RBSE '98

18 **The Connection Between Sunspots and Power Outages**
Natasha Feden and Alicia John
Chenery Middle School, Belmont MA
Teacher: Elizabeth Chait-Sanghavi, RBSE '98

(Continued on next page)

Table of Contents (continued)

Nova Research:

22 **A Search for Novae in the Andromeda Galaxy - Year Two Results**
Ken Phelps, Catherine Provenzano and the Nova Search 2000 Research Group
Grosse Pointe North High School, Grosse Point, MI
Teacher: Ardis Maciolek, RBSE '98

26 **The Correlation of the Location of Novae in the Andromeda Galaxy with Respect to the Duration of their Light Curves**
Matt Harriger
Harry A. Burke High School, Omaha, NE
Teacher: Tom Gehringer, RBSE '98

30 **The Search for Novae in the M31 Galaxy**
Ben Nascenzi
Cranston East High School, Cranston, RI
Teacher: Howard Chun, RBSE '99

AGN Research:

p. 32 **The Correlation of Active Galactic Nucleus Type with Distance as Determined by the Redshift of Spectral Signatures**
Ryan Westerlin
Harry A. Burke High School, Omaha, NE
Teacher: Tom Gehringer, RBSE '98

p. 38 **Investigating and Categorizing AGN Objects**
Karyn Beaudry, Stephanie McClain, Ryan McCusker and Ethan Robinson
Cranston East High School, Cranston, RI
Teacher: Howard Chun, RBSE '99

Sunspots and Earthquakes

José Santiago
Sabana Llana Middle School, Río Piedras, Puerto Rico
Teacher: Maria Hernández, RBSE '99

Abstract

My science teacher, Mrs. Hernández, attended an astronomy workshop at the National Optical Astronomy Observatory (NOAO) in Arizona. When school started, she got us involved in the project, and I was motivated to carry out this investigation. I was interested in astronomy, particularly, in solar activity, and I asked myself if there was a relationship between the number of sunspots and earthquakes. Personally, I l believe there is, so I started my investigation with the help of the solar telescope prepared at NOAO, a CD-ROM that processes images from RBSE (vacuum telescope at Kitt Peak, Arizona), and the Internet. I studied sunspots and earthquakes from 1989 to 1998. I made a list of the earthquakes that occurred during that decade and the number of sunspots, three months before and three months after each earthquake. After analyzing data, my hypothesis was correct. Data seems to support that there is a connection between the number of sunspots and the occurrence of earthquakes, therefore, I plan to repeat this investigation next year, improving data and increasing the number of earthquakes to be studied.

Introduction

I was motivated to carry out this investigation after my science teacher received a seminar in astronomy at the National Optical Astronomy Observatory (NOAO). I was interested, particularly, in solar activity. I started asking myself whether there was any relationship between the number of sunspots and earthquakes. I think there is, therefore, I chose this topic.

Problem

Is there a relationship between the number of sunspots and earthquakes?

Hypothesis

I think there is a connection between the number of sunspots and the occurrence of earthquakes.

Methodology

From the yard of my school, I started a day by day count of the number of sunspots with the help of a solar telescope made at NOAO. Then I made a deeper study of sunspots with the help of a CD-ROM that processes images from the RBSE (vacuum telescope in Kitt Peak, Arizona). From these images I studied the latitude, the longitude, the measure of sunspots and how long they lasted. Afterwards, I went on the Internet at web sites: http://science.msfc.nasa.gov/ssl/pad/solar/greenwch/spot_num.txt and http://www.neic.cr.usgs.gov/neis/eqlist/last_big10.html. From these web sites I obtained a list of the earthquakes that took place from 1989 to 1998, and the number of sunspots three months before and three months after each earthquake. Then I prepared a graph to investigate if there was any connection between the number of sunspots and the occurrence of earthquakes.

Conclusion

According to the analysis of data, in 9 out of 10 earthquakes studied, there was in an increase in the number of sunspots before the earth's movement. Data seems to support my hypothesis that there is a connection between the number of sunspots and the occurrence of earthquakes.

Projections

Next year, I plan to repeat this investigation (Phase II) in order to do further research on this topic, nevertheless, I will try to improve data. First, I will include the month in which the earthquake took place, and I will also increase the number of earthquakes to be studied.

References

http://science.msfc.nasa.gov/ssl/pad/solar/greenwch/spot_num.txt

http://www.neic.cr.usgs.gov/neis/eqlist/last_big10.html

RBSE CD-ROM v4.0

Solar Telescope National Optical Astronomy Observatory (NOAO)

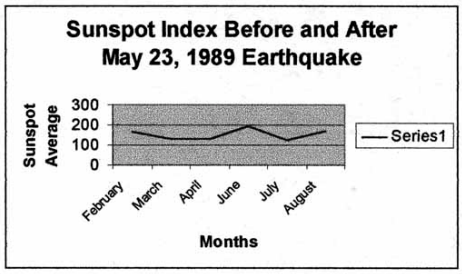

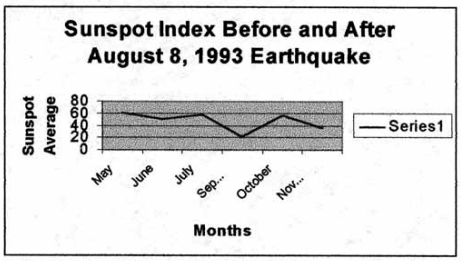

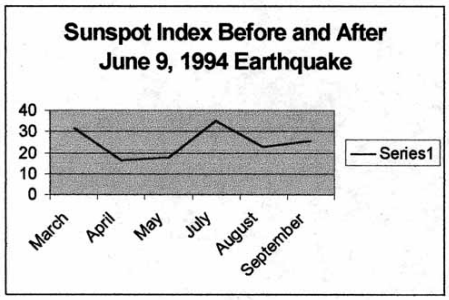

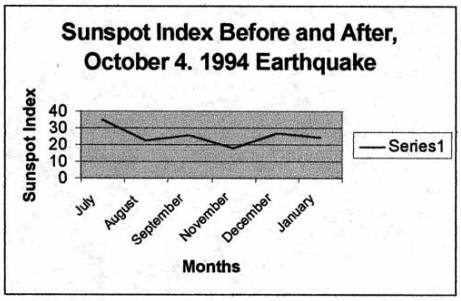

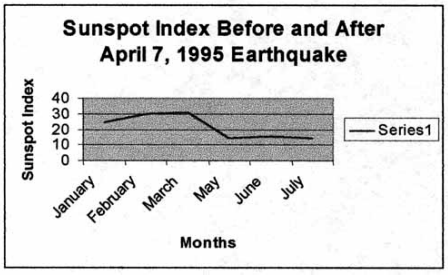

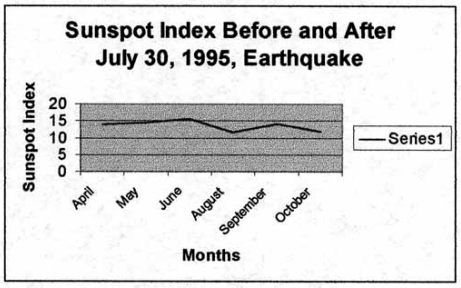

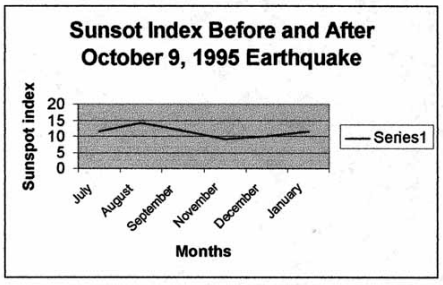

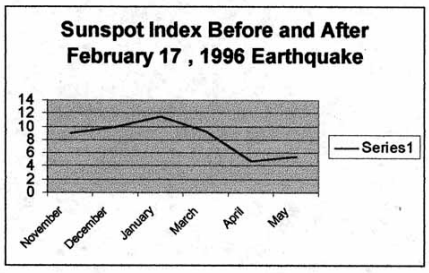

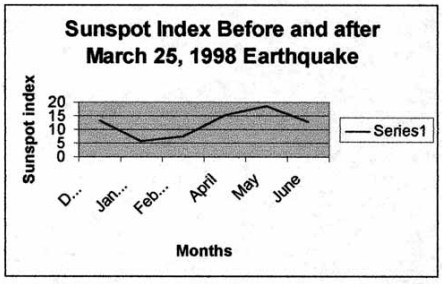

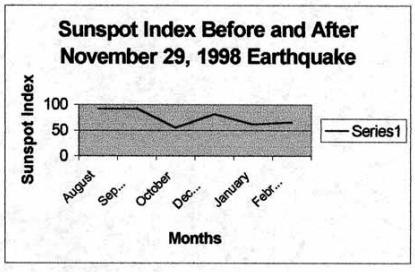

Sunspots and Hurricanes

Carlos F. Ramírez
Sabana Llana Middle School, Río Piedras, Puerto Rico
Teacher: Maria Hernández, RBSE '99

Abstract

Last summer our professor María Hernández attended a workshop on sunspots at Kitt Peak, Arizona. From the knowledge acquired at this workshop, she started to develop with us a project to study sunspots. She gave us a workshop on how to use the solar telescope and the data we obtained from it. These experiences and, given the fact that each and every year, during hurricane seasons, our island has to be alert to these atmospheric phenomenons, I was motivated to investigate if there was a connection between these and sunspots. I based my investigation over a period of twenty-one (21) years, from 1979 to 1999, making use of the solar telescope and the Internet, studying sunspots and hurricanes with the objective of establishing a relationship between both. After analyzing data, I conclude that sunspots do not affect the amount of hurricanes. Nevertheless, I look forward to contune studying sunspots because they could explain other phenomena that affect our planet.

Introduction

This project comes forth after Mrs. María Hernández, our science teacher, gave us a workshop on how to use a solar telescope and how to manage the data we obtained from it. The hurricanes of the past seasons intruiged me a lot, and so I decided to investigate if sunspots had any effect on the amount of these atmospheric phenomena that occur each year. I based my investigation over the last twenty-one (21) years, from 1979 to 1999, hoping that results answer my question of whether sunspots affect hurricanes.

Problem

Is there a relationship between sunspots and the ammount of hurricanes that occur yearly?

Hypothesis

Sunspots affect the amount of hurricanes that take place each year.

Methodology

For this investigation, I studied sunspots with the solar telescope. Then I used a CD-ROM from NOAO (National Optical Astronomy Observatories) to obtain information about sunspots. After that, I went on the Internet to seek information about the hurricanes that had taken place throughout the years 1979 to 1999; obtaining a list that included dates, air pressure, and categories. I looked for additional information on sunspots to be able to analyze the amount of these in relation to the amount of hurricanes in the past twenty-one (21) seasons. I compared the data making use of charts and graphs.

Data Analysis

Data indicates that there is no connection between sunspots and the amount of hurricanes in the different seasons. As it can be observed, in seasons where there were a greater or less number of hurricanes also reflected a greater or less number of sunspots, indistinctly. It can't be established, therefore, that to a greater or lesser number of sunspots there is a greater or lesser number of hurricanes. In other words, in seasons where there were many hurricanes (up to 19), data reflects few sunspots in some seasons, and a greater number of them in others. The same happens in season where there were a small number of hurricanes.

Conclusion

Having analyzed data and obtained the results of my investigation, I conclude that there is no relationship between sunspots and the amount of hurricanes that can occur each year. In other words, that the number of sunspots has no effect on the amount of hurricanes in a season.

Projections

I consider that this investigation is of great importance because it allows the study of the relations between sunspots and atmospheric phenomena. Nevertheless the results of my investigation, I am still interested in studying sunspots and their relationship, if any, with hurricanes from other aspects, such as: density and water vapor. On the other hand, I expect to investigate if there is any relationship between sunspots and other phenomena that affect our planet; for example, solar radiation.

References

http://koa.ifa.hawaii.edu/ARMaps/Yesterday/990906.1632_armap.gif

http://weather.unisys.com/hurricane/atlantic/

http://www.nso.noao.edu/synoptic/

SunSpotter II (Solar Telescope): National Optical Astronomy Observatories

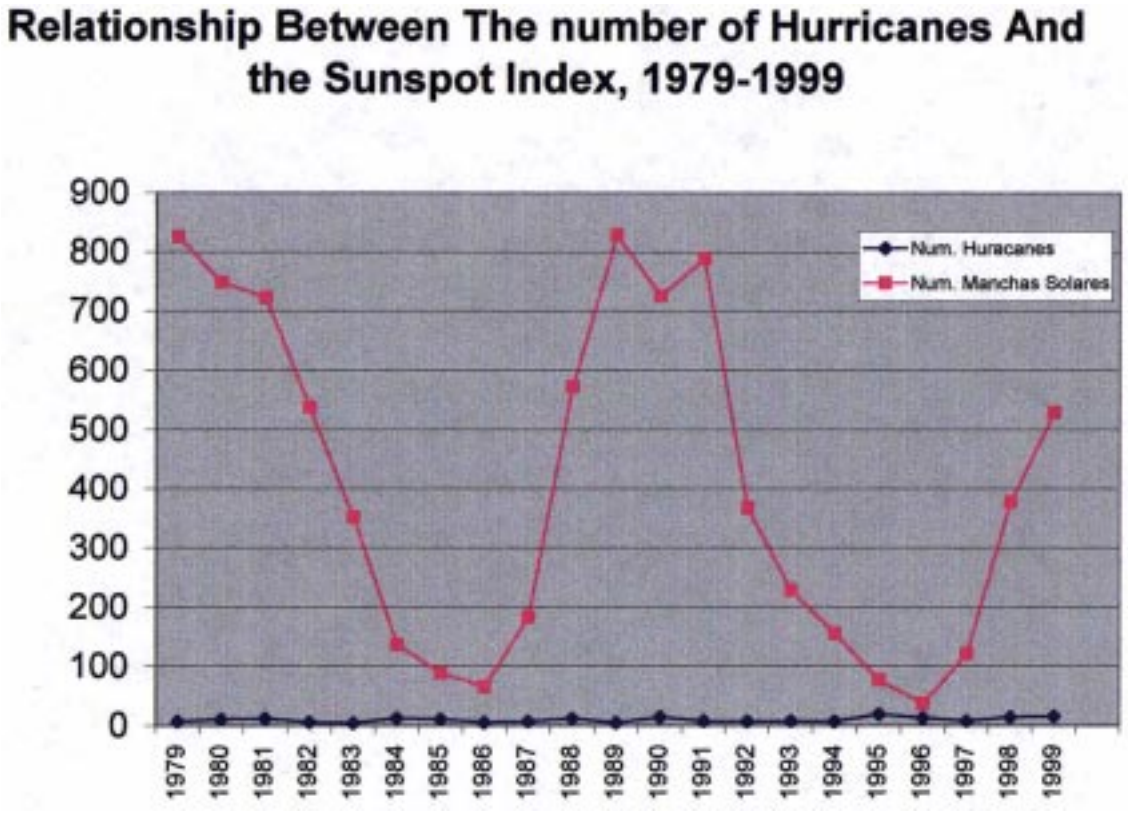

Identifying Unknown Solar Absorption Lines

Todd Faner and Regan Wilson
Grosse Pointe North High School, Grosse Point, MI
Teacher: Ardis Maciolek, RBSE '98

Abstract

Sections of the solar absorption spectrum from 3400-6270 Angstroms were examined by using an on-line database to find absorption lines that were unidentified. By querying the Vienna Atomic Line Database, a synthetic solar spectrum was created. The comparison between the synthetic and actual absorption lines revealed solar lines that were identified as specific elements. Features were evaluated to determine if they were blends and their positions verified with respect to known lines. Some previously- identified lines were revised. Seventeen new identifications and forty-four revisions were discovered.

Introduction

Despite one hundred years of research into the solar spectrum, there are still many absorption features that have not been identified. These absorption features directly correspond to identities of elements. Since the last time (1970's) that major identifications were made on these lines, much work has been done on all the of the atomic spectrum, especially recently with new line identifications being made in the Rare Earth and transition elements. This project used a synthetic spectrum to identify unknown absorption lines in the real spectrum of the sun.

Hypothesis

Previously unknown absorption lines of transition metals and rare earth elements in the sun can now be identified. In addition, all solar models currently factor out unidentified lines. These new identifications will affect the elemental abundance estimates so future solar models will have to be revised.

Procedure

The first step of the process was to meet with Professor Donald Bord of the University of Michigan and learn generally about the solar spectrum and how to identify elements by their absorption lines. Professor Bord then explained how to submit a query to the Vienna Atomic Line Database (or the VALD).

The VALD is a collection of atomic line parameters of astronomical interest and it also provides tools for selecting subsets of lines for typical astrophysical applications: Line identification, chemical composition and radial velocity measurements, model atmosphere calculations, etc. In addition, the BASS 2000 web site, and the Photometric Atlas of the Solar Spectrum could be used to examine the lines in the current spectrum.

After examining the solar spectrum the query starting point was placed in the ultraviolet range, because the line density is greater and there are more unidentified features. This area also has less telluric lines, absorption bands that are caused by molecules in the Earth's atmosphere. Since these aren't caused by the photosphere of the sun, using them in the data is out of the question because they are distinctly a foreign piece of information. Also, they are molecular or polyatomic bands, so their activity clearly differs from that of the atomic lines in the sun.

With all this in mind a query to the Vienna Atomic Line Database (VALD) was made through the use of email. Using "Extract Stellar" mode, the default parameters were solar, so few changes needed to be made. VALD would create a synthetic spectrum for the portion queried, with all lines identified, according to their known behavior on Earth. This would allow the unidentified features in the solar spectrum to be identified.

Data

Ten separate queries were made to the VALD, three of which were returned to be unusable. The data were returned

without any lines and a message that that portion of the spectrum was unusable. The first queries were made in the lower regions, or ultraviolet, and the queries would go higher up each time, ending with a spot just below the infrared range. The areas in the green portion of the visible light were determined unusable. There were too many large absorption features. The large absorption features block out the smaller unidentified lines, making them truly unidentifiable. The whole data spreadsheet was seventeen pages, so for the purposes of this paper, two shorter spreadsheets were created. The first has all the newly- identified lines, and the second lists lines believed to be incorrectly identified in the original published research, along with their proposed new identities.

For each spreadsheet, the first column has the observed line position in angstroms. The second column has the line position of the created spectrum in angstroms. And the third column has the difference between the two. The next is the elemental identification column. This gives the element and its ionization number. The ionization number of one is neutral, number two would be missing one electron, number 3 would be missing two electrons, etc.

New Solar Line Identifications

Observed Features Wavelength (Å)	Virtual Features Wavelength (Å)	Query Difference Wavelength (Å)	Elemental ID
3400.232	3400.25	0.018	Ce 2
3401.344	3401.343	-0.001	V 1
3401.858	3401.859	0.001	Os 1
3410.791	3410.797	0.006	Mn 1
3411.977	3411.958	-0.019	Ni 1
3416.782	3416.69	-0.092	Fe 2
3420.598	3420.601	0.003	Ni 2
3427.522	3427.556	0.034	Fe 1
3430.955	3430.91	-0.045	Co 1
3431.072	3430.979	-0.093	Gd 2
3431.185	3431.189	0.004	Tm 2
3435.593	3435.546	-0.047	Sc 1
3439.872	3439.828	-0.044	Ce 2
3446.612	3446.605	-0.007	Ti 1
3499.269	3499.255	-0.014	Ni 1
6265.6	6265.612	0.012	Mn 1
6269.977	6269.967	-0.01	Fe 2

Analysis

After a week's turn-around time for each VALD query, the synthetic spectrum was compared to the actual spectrum. The features in the observed spectrum were matched to their corresponding lines in the virtual spectrum. To identify the unknown lines, a graph of that portion of the spectrum would be obtained using the Photometric Atlas of the Solar Spectrum, a reference book that plotted the entire spectrum on paper and the BASS 2000 web site. This web site had the entire spectrum online. The position and range of the portion in question could be changed in seconds, saving valuable time.

Solar Line Revisions

Observed Features Wavelength (Å)	Virtual Features Wavelength (Å)	Query Difference Wavelength (Å)	Previous Elemental ID	New Elemental ID
3400.019	3400.106	0.087	Gd 2	Cr 2
3401.173	3401.067	-0.106	Ni 1	Gd 2
3401.530	3401.538	0.008	Fe 1	Ni 1
3402.074	3402.071	-0.003	Co 1	Gd 2
3402.552	3402.564	0.012	NH	V 1
3402.900	3403.081	0.181	Zr 2	Gd 2
3403.271	3403.271	0	Fe 1	Th 1
3404.31	3404.3539	0.0439	Mo 1	Fe 1
3405.371	3405.205	-0.166	NH	Cr 1
3406.121	3406.094	-0.027	NH	Ca 2
3408.505	3408.447	-0.058	Fe 1	Ca 2
3409.671	3409.588	-0.083	Co 1	Fe 1
3409.948	3410.01	0.062	NH	Cr 2
3412.887	3412.865	-0.022	NH	Co 1
3413.270	3413.275	0.005	NH	Gd 2
3413.410	3413.471	0.061	Zr 2	Ni 1
3413.650	3413.652	0.002	NH	Fe 1
3415.443	3415.429	-0.014	Cr 2	Fe 1
3416.512	3416.566	0.054	Fe 1	Ce 2
3416.869	3416.857	-0.012	Fe 1	Ce 2
3417.066	3417.058	-0.008	NH	V 1
3417.359	3417.273	-0.086	Ru 1	Cr 1
3420.108	3420.17	0.062	NH	Fe 2
3422.496	3422.499	0.003	Fe 1 (Gd 2)	Co 1
3422.759	3422.753	-0.006	Cr 2	Gd 2
3422.759	3422.759	0	Ce 2	Co 1
3423.715	3423.704	-0.011	Ni 1	Ni 1
3423.839	3423.838	-0.001	Co 2	Ni 1
3423.994	3423.989	-0.005	Fe 1	Ni 1
3424.713	3424.613	-0.1	NH	Re 1
3425.446	3425.305	-0.141	Fe 1	Ni 1
3426.912	3426.988	0.076	NH	Fe 1
3427.612	3427.72	0.108	Cr 1	Ni 1

If the lines had double-peaks, round tips, misshapen slopes, fat bottoms, or were asymmetrical at all, the VALD identification could not be taken as absolute. These blends, or features that are more than one line near the same position, that add together to produce an asymmetrical feature. Blends were ruled out and taken as unidentifiable.

The position of the VALD line would need to have an acceptable agreement in position with the observed line, and the unknown observed line would need to have the correct placement between two known features, to assure it was a single line, and be good-looking. If these checks had passed, the VALD's identification of the line could be assured as proof positive.

The differences between the position of the lines in the query and the actual spectrum were recorded on the "identified lines" spreadsheet.

There were lines in the observed spectrum already identified in 1966, but the VALD definition of the line disagreed. In some cases, the observed feature would have a question mark after it. This indicated that the line was thought to be of that identification, but it wasn't an absolute. The lines where this occurred were Fe 1 or Fe 2. In the past decade, there have been intensive studies on the iron lines in the solar spectrum in Sweden. Since the VALD is updated to this, and the observed features book is rather outdated, the VALD definition was taken. On lines that didn't agree, and didn't have a question mark after them, the lines bracketing that feature were examined. If they were identified in both the VALD and the observed spectrum, and, were an acceptable distance away from the line in disagreement, then the VALD definition was taken. If the line didn't meet the above parameters, the observed definition was taken, because the VALD could not be used unless it was without a reasonable amount of error. The solar spectrum research was dated 1966, and the VALD model has revisions made, as of the 1993 solar model. This is the reasoning behind favoring the VALD definition during disagreements.

The differences in line positions of the observed and virtual spectra were figured next. This was easily accomplished by subtracting the observed from the virtual. Using this, the standard deviation was calculated for the observed and virtual spectrum's known and newly identified line differences. Standard deviations of the differences from the known versus the newly identified lines were compared. The standard deviations of the new identifications were smaller than and in good agreement with the standard deviations of the known lines.

The standard deviation derived from all the known lines was 0.047. The standard deviation from all the newly-identified lines was 0.035.

After counting the number of unidentified lines in the sun, they totaled 6126 lines. Factoring in the seventeen lines which were identified by this research, the change in the number of unidentified lines in the solar spectrum is 0.28%.

Conclusions

Seventeen new lines were identified: rare earth elements (cerium II, gadolinium II, thallium II) and transition metals (vanadium I, osmium I, manganese I, nickel I&II, iron II, cobalt I, scandium I, and titanium I) were found. This caused a change in the number of unidentified lines in the solar spectrum of 0.28%.

Forty-three line identifications were revised involving thirteen transition metals and four rare earth elements. Because of the discoveries of these new and revised lines, changes will have to be made to the current solar model.

Extensions

In the future, the plan will be to process more queries, and identify more elements. This will provide even more evidence of how the current solar model needs to be revised. A next step will be to calculate the abundances of these newly identified elements.

Bibliography

Delbouille, L., Neven, L., Roland, G. Photometric Atlas of the Solar Spectrum from 3000 to 10000. The Institut d'Astrophysique de l'Universite de Liege, Conite-Ougree, Belgium: 1973.

High Resolution Solar Spectrum: http://mesola.obspm.fr/form_spectre.html

Moore, Charlotte E., Minnaert, M.G.J., Houtgast, J. The Solar Spectrum 2935 A to 8770A. National Bureau of Standards Monograph 61, Dec. 1996.

Online Solar Line Database: ftp://astro.lsa.umich.edu/hub/get/bord

Vienna Astrophysical Line Database: plasma-gate/weizmann.ac.il/VALD.html

The Effect of Sunspots on Temperature and Ultraviolet Rays

Jessy Farrell, Heather McPherson, and Yasmin Afsar
Chenery Middle School, Belmont MA
Teacher: Elizabeth Chait-Sanghavi, RBSE '98

Abstract

Our group was interested in the effect sunspots have on Earth. We decided to focus on two subjects: temperature and ultraviolet (UV) rays. When we started this project, we hypothesized that when the sunspot index rises, both temperature and the UV ray index would rise as well. We show that temperature does rise and fall with the sunspot index, but that the connection between the UV index and sunspot index is weaker. To help us find information, we decompressed images on WinZip from Kitt Peak Solar Observatory, and analyzed them on Scion Image.

Introduction

We wanted to find out if the sunspot index affected both the UV index and the average annual global temperature on Earth. Our hypothesis was that the greater the sunspot index, the greater the UV index and the average annual global temperature. During a sunspot minimum, we think that the Earth's average annual temperature will decrease, and more UV rays will escape the sun. Heat and radiation will thus affect the Earth.

Most people looking for the cause of global warming have pointed to the greenhouse effect. They have missed some crucial scientific data: the radiation from the sun is not constant. This fact is important because climate models used by greenhouse theory proponents used to assume that the sun's radiance was constant. With this thought in hand, they could ignore solar influences.

The assumption that the sun's radiance is constant is not valid. Further research revealed a strong connection between global temperature on Earth and sunspots. When a solar minimum occurs, temperature on Earth is cooler, with the opposite occurring during a maximum. Researchers point out that the half degree rise in global temperature over the last 120 years occurred before 1940, before the sharp increase in greenhouse gas emissions that has taken place over recent decades. Also, using ancient tree rings, scientists can show that seventeen out of nineteen warm spells in the last 10,000 years coincided with peaks in solar activity.

The little ice age, from 1650 to 1850, affected mostly the Northern Hemisphere. Temperatures in this period fell 2°F below today's average temperatures, causing canals in Venice to freeze, glaciers to advance, and major crop failures. This happened during a time when the sun was at a solar minimum. From 1645 to 1715, the sun was in a stage referred to as the Maunder Minimum. During this time, the sun had few spots and little magnetism.

When the sun began to emerge from this minimum in the early 1700's the Earth warmed up, ending the little ice age. Since 8,700 B.C., there have been ten major cold spells, similar to the Maunder Minimum. Nine of these cold spells have coincided with a sunspot minimum.

Changes in the sun's radiation strongly affect the Earth and contribute to global warming. One widely discussed connection is the effect of the sun's radiation on components of the Earth's atmosphere. Since sunspots give off UV radiation, we assumed that the greater the sunspot index, the greater the UV index.

Ultraviolet radiation is one of the components of the light spectrum. It has many effects, not only on humans but on other natural features. For example, coral reefs turn beautiful colors when exposed to UV radiation. Excess exposure to UV radiation is considered harmful to human health. It is associated with skin cancer, cataracts, and other diseases. Exposure to UV radiation is more intense at higher altitudes and many pilots are becoming concerned about the potential health hazards they face because of their work.

Our research did not reveal many studies on the connection between the sunspot index and UV rays on Earth. We hope that our project will stimulate a series of other studies that will help improve knowledge about this relationship.

We decided to explore the relationships between sunspots and global temperature and UV rays because of their potentially bad effects on the Earth. A rise in the sunspot index may lead to higher temperatures and greater radiation exposure on Earth.

Methods

There were many difficult but rewarding moments during this project. When we first learned to use WinZip32 to download images, and to use Scion Image, we were unsure of ourselves. These programs are used to analyze images of the sun. WinZip32 decompresses the images, and Scion Image allows us to analyze them. Now that the project is over, we are experts at using these programs to find sunspot indexes.

For information on UV rays, our group wrote to a commercial firm asking them what units they used in their UV index data tables. Their response was not helpful. On the Internet, we found a wide range of sites when we searched the topic of "UV data" and "historical temperature." We were excited to find the information and printed out much of it to improve our understanding of the data and to determine what connections there may be between the series.

Results

The basic data set we assembled is reported below. For selected years starting in 1856, the data cover the average annual global temperature, the sunspot index, and (when available) the UV index. What these data show is a relatively strong association between sunspots and temperature.

These data provide support for both of our hypotheses. During periods when the sunspot index was high, the temperature and UV index were greater than they were when the sunspot index was at a minimum. For example, in 1996, 1997, and 1998, the sunspot indexes were 8.6, 21.5, and 64.3, respectively. The average temperatures for those three years were 14.22, 14.43, and 14.57 degrees Celcius. The UV indexes also rose, 267.6951, 271.7949, and 278.6275.

The three indexes generally rose and fell together. In 1996, a sunspot minimum, the average temperature was 14.15 degrees Celsius, lower than it was in 1999, at 14.5. The sunspot indexes for those two years were 23 and 70, respectively. Looking at our long-term data, we can see clearly the 11-year cycles. When the sunspot index rises, so does the temperature on Earth. From this pattern, we can predict warm weather this year.

Conclusion

Based on our data, we can conclude that the sunspot index does affect both average annual global temperature and the UV Index. The evidence shows support for our hypothesis that it would be colder on Earth during a sunspot minimum and warmer during a sunspot maximum. There is also evidence that a rise in the sunspot index is associated with a rise in the UV index.

In the abstract, we noted that the UV index increased when the sunspot index increased but that the relationship was weaker. During 1995, the sunspot index decreased to 17.5 while the UV index increased to 307.043. This was an odd result but we did not believe that it was reason to doubt the overall trend in the data.

YEAR	TEMPERATURE (degrees C)	SUNSPOT INDEX	UV INDEX
1856	13.64	4.3	-
1857	13. 53	22.7	-
1858	13.58	54.8	-
1859	13.77	93.8	-
1860	13.6	95.8	-
1861	13.59	77.2	-
1862	13.47	59.1	-
1863	13.74	44	-
1864	13.54	47	-
1865	13.75	30.5	-
1866	13.8	16.3	-
1867	13.69	7.3	-
1868	13.8	37.6	-
1869	13.71	74	-
1870	13.68	139	-
1871	13.64	111.2	-
1872	13.79	101.6	-
1873	13.72	66.2	-
1874	13.6	44.7	-
1875	13.57	17	-
1876	13.59	11.3	-
1877	13.87	12.4	-
1878	13.99	3.4	-
1879	13.71	6	-
1880	13.72	32.3	-
1885	13.66	52.2	-
1890	13.61	7.1	-
1900	13.86	9.5	-
1910	13.54	18.6	-
1920	13.77	37.6	-
1930	13.85	35.7	-
1940	13.98	67.8	-
1950	13.8	83.9	-
1960	13.99	112.3	-
1970	13.97	104.5	-
1980	14.1	154.6	-
1990	14.34	142.6	-

1991	14.29	145.7	-
1992	14.15	94.3	-
1993	14.19	54.6	-
1994	14.26	29.9	226.346
1995	14.38	17.5	307.043
1996	14.22	8.6	267.6951
1997	14.43	21.5	271.7949
1998	14.57	64.3	278.6275
1999	14.1	93.4	310.0826

Sunspots and Flight Safety

Kirby Tyrrell, Catherine Caruso and Emilie Anderson
Chenery Middle School, Belmont MA
Teacher: Elizabeth Chait-Sanghavi, RBSE '98

Abstract

How the sunspot number affects the safety of air travel was studied. Research was conducted to determine if during the solar maximum pilots have more trouble navigating airplanes than at any other time. The hypothesis for this question was that the chances were higher of crashing during the solar maximum. After doing a substantial amount of research using the Internet, the phone, and Scion Image, the hypothesis was proved correct.

Introduction

Research on how the sunspot number affects flight was conducted. The question asked was, is it more difficult to navigate airplanes during the solar maximum than any other time? The hypothesis for this question was that during the solar maximum, airplanes are affected more and the number of navigational problems (crashes) does increase.

To help investigate the question, information was found on the Internet on how planes navigate. Planes are controlled by three methods, pilotage, dead reckoning, and radio navigation. Pilotage is the simplest way of navigating; it is when the pilot keeps on course by following landmarks. Before taking off the pilot makes an aeronautical chart to show landmarks. When he passes over them, he checks them off on the chart. If he does not pass directly over them, he knows he is off course. This method of navigation could not be affected by solar activity because it is not controlled by power-driven instruments such as radios or satellites.

The second method of navigation is dead reckoning. This method is used when there are few or no perceptible landmarks. This method is more complicated than pilotage. In this method the pilot does need instruments, one could use a clock, compass, and a small computer for figuring out difficult math problems. The pilot uses a chart to plan a route before he flies. He also calculates how long it will take to reach the target if he flies at a constant speed. The computer allows the pilot to revise his course in case there is wind. If the plane is over a location at the correct time the pilot knows he is on course. Since the pilot does use instruments such as a compass it could be affected by sunspots, this navigational method is more risky during the solar maximum. Geomagnetic storms could affect the magnetic north, on which the compass is based.

The third method of navigation is radio navigation. Airplanes use radio systems named LORAN and OMEGA. These systems are heavily affected during solar maximums since solar activity can upset radio wavelengths. The OMEGA system contains eight stations throughout the world. Airplanes receive very low frequency signals from these stations to determine their positions. During solar activity, the station can give incorrect information to navigators causing them to be three or four miles off course. If pilots are aware of a solar storm, they will switch to a back-up system, but sometimes they are not alerted fast enough. This is how sunspots can affect air navigation.

Methods

To begin the project, the FAA, The Federal Aviation Administration was called. In speaking to Net Preston, a historian at the FAA, information on number of planes that had crashed out of the number launched during the years 1997 and 1999 in the months January, May, and September was obtained. To interpret the data more easily, it was first put into a ratio to find the percents. Then it was converted into fractions over 100,000 so that the numbers would be more understandable.

The next step was to find the sunspot index for the same months and years as the crash data. This step was completed using Scion Image to analyze images from the Kitt Peak Observatory in Arizona. The fifth day of each month was used to find an average. This was the research that took the longest, because there were many sunspots to count.

There was also a great deal of information on the Internet that assisted in writing the introduction of this report. It is helpful that this year is the solar maximum because there seems to be a lot more information on the Internet than other years. All of these factors helped in writing the report.

Results

See graphs attached

Conclusion

From the data, one can conclude that sunspots do influence the navigation of airplanes and they may increase the number of plane crashes in the United States. In January 1997 the sunspot index was 5.6 and the number of plane crashes per one hundred thousand planes launched was only 3.3. In January 1999, the sunspot index was 44.4 and the number of plane crashes per one hundred thousand was 4.8. During the month of May 1997, the sunspot index was 11.6 and the number of plane crashed was 5.8. Then during May 1999 the sunspot index was 62.5 and the number of plane crashes was 11.6. During the month of September 1997, the sunspot index was 19.4 and the number of crashes was 5.3. During September 1999 the sunspot was 71 and the number of plane crashes per one hundred thousand was 11.5. From this data, there appears to be a relationship between the sunspot index and plane crashes. For almost every month when the sunspot index became higher, the number of plane crashes rose as well. It also proves that the hypothesis was correct.

One complication to the project was that starting in May 1997 the number of plane crashes decreased and kept decreasing until January 1999. Since it is unknown what happened in 1998 a conclusion cannot be made about why this happened. This is the only problem encountered during this project.

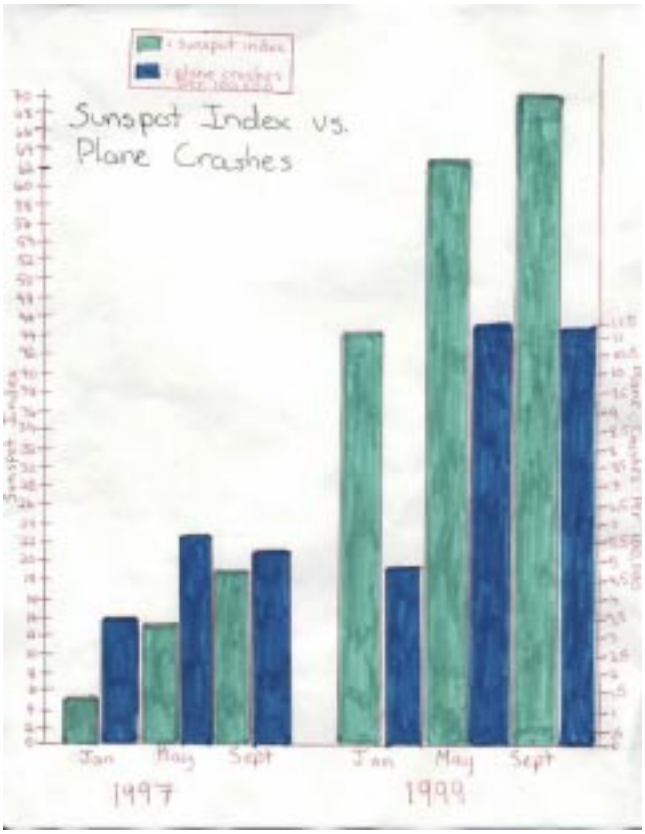

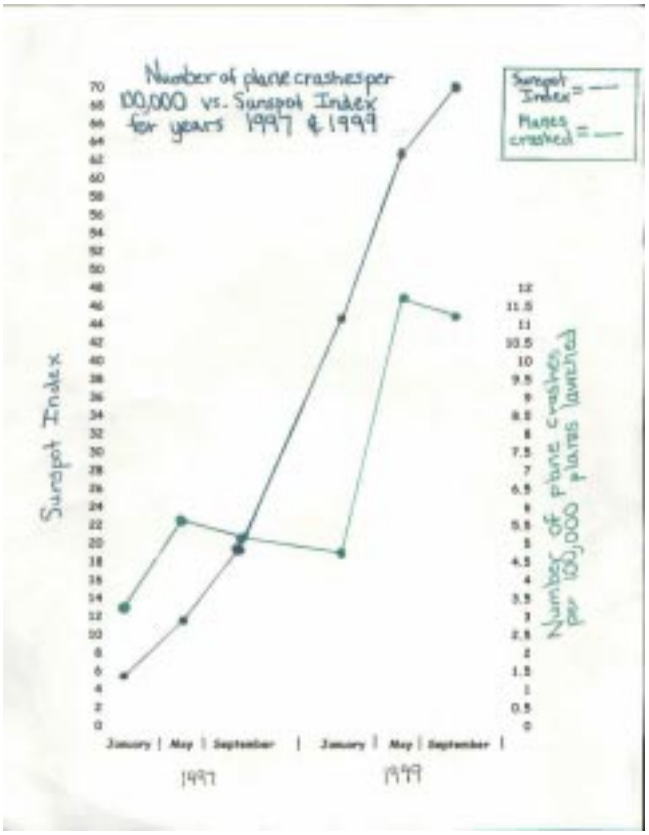

The Connection Between Sunspots and Power Outages

Natasha Feden and Alicia John
Chenery Middle School, Belmont MA
Teacher: Elizabeth Chait-Sanghavi, RBSE '98

Abstract

We have frantically searched for information on how the number of sunspots affect the number of power outages. Our hypothesis was that the number of sunspots did affect the number of power outages. We used the Internet, Scion Image, WinZip, our computer lab at school and Ms. S. We feel that we proved our hypothesis very well.

Introduction

We did a project on the connection between the sunspot index and the number of power outages.

Power outages affect our daily lives. People use power to cook, run the dishwasher and refrigerators. We also use it for light, entertainment (watching TV), communication (telephones) and computers. They want to be able to predict power outages. If researchers and scientists were able to grant us that, people would prepare themselves with flashlights, candles and batteries. Maybe understanding the connection will help people be prepared in their daily lives.

We think that the answer to our question will be that more sunspots cause more power outages. We think this because sunspots cause solar flares/winds that cause the radios to have static. Maybe more solar wind/flares will cut off the power also.

Sunspots are disturbances on the sun's surface. They look like dark regions on the sun in pictures. They look dark because they make the area around them is cooler. Sunspots follow an 11 year cycle. During those 11 years, there is a solar maximum and solar minimum. A solar maximum is when the sunspot index is the highest. The year 2000 is a solar maximum. Therefore, our question will be of particular concern this year. The solar minimum is when there is the least number of sunspots. The most recent minimum was in 1996.

The more sunspots there are, the more likely we will have solar flares. Solar flares are bursts of magnetic energy that shoot up from the sun. Huge amounts of heat and light are given by these flares that turn into solar winds. If this energy reaches Earth, it can affect Earth's magnetic field and disrupt radio reception.

We believe that sunspots cause power outages because in March 1989, a geomagnetic storm hit Quebec Hydro Power System. This caused the power to go out for more than twelve hours. This occurred during a solar maximum.

Methods

We used KPVT data to find our information on sunspot indexes for February, July, and November. We chose these months because we wanted to do the beginning, middle, and end of each year. December and January were too close to each other so we did February and November. KPVT data are images of the sun taken from a vacuum telescope in Kitt Peak, Arizona. We chose the years 1996 and 1999 because they were the sunspot minimum and close to the sunspot maximum respectively.

To view KPVT data, we first had to decompress the files. WinZip extracts the files so that we can look at them. Scion Image helped us to view our data and find the sunspot index. We used the formula 10 times the number of groups plus the number of sunspots to find the sunspot index.

We also went on the World Wide Web. We found a website about sunspots which gave very good background information. The website was http://www.fcc.gov/Bureaus/Engineerng_ Technology/Filings/Network_Outage/1996/report.html. Or you could have 1999 instead of 1996. Next, we discovered a website listing major power outages. We got them for 1996 and 1999. We e-mailed Robert K. (the author of the website) but he was unable to help us.

Results

See attached graphs and tables.

Conclusion

We will share our conclusion drawn from the previously stated data. Notice that the number of power outages in 1996 is 14. In 1999 it is 22. That is nearly double. In February, notice that in 1996 the average sunspot index is 0. However, in 1999 it is 43.6. The key data is that when the sunspot index is high with an average of 63.23 in 1999, the power outages become more frequent, with a total of 51 outages in three months. However, we noticed that in 1996, where there was a sunspot index average of 6.77 the number of power outages decreased by about 6 less outages!

We received an e-mail from Robert K. of the Federal Communications Commission, and author of website on outages, that the power outages were really telephone outages. After a day of panic, we pointed out that telephones use electricity. When Ms. S. said that what we had was all right we were so relieved. That was only one of the many problems. Another problem was that if we raised our hand, Ms. S. was not always available to help us until it was time to go. This meant that we had to think of answers to some of the questions on our own. A third problem is that our schedules conflicted and we could not get together often. This caused some of us to "zone out" and get irritated with one another. This also caused us to work on some parts of our project alone. A fourth problem was that in the beginning when we started this project, it took us a whole period to open up 1 image of the sun on Scion Image. We solved this last problem with a lot of practice! Now we can get an image in 10 seconds.

We would have changed this project by doing a different question! This question is incredibly hard to prove, because we can not go around the world asking people if they had power outages. Even if we could, we would have to subtract the power outages that were caused by blizzards or winds knocking down telephone poles. It is really impossible to be absoloutely sure of what caused each power outage. Then we would have to say that it was in a solar maximum and prove that the sunspots caused it.

To solve the time problems, we should have a schedule where we will have 3 minutes when we can ask Ms. S. questions. We should also plan ahead and set certain times where we can get together. Now our conclusion comes to an end. But, be prepared for power outages this year. Especially since April is the maximum of the maximum.

AVERAGE SUNSPOT INDEX		
	1996	**1999**
February	0	43.6
July	7.3	72.8
November	13	78.3
Total Averages	6.77	63.23

POWER OUTAGES		
	1996	**1999**
February	17	11
July	14	22
November	15	18
Total	46	51

THE NUMBER OF POWER OUTAGES AND SUNSPOT INDEX FOR JULY 1999

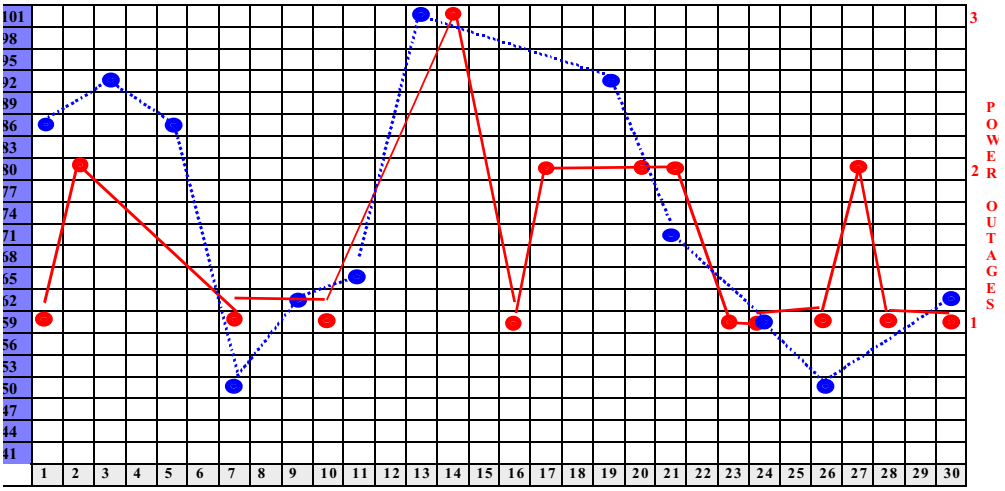

JULY 1999

Power Outages

Sunspot Index

THE NUMBER OF POWER OUTAGES AND SUNSPOT INDEX FOR NOVEMBER 1999

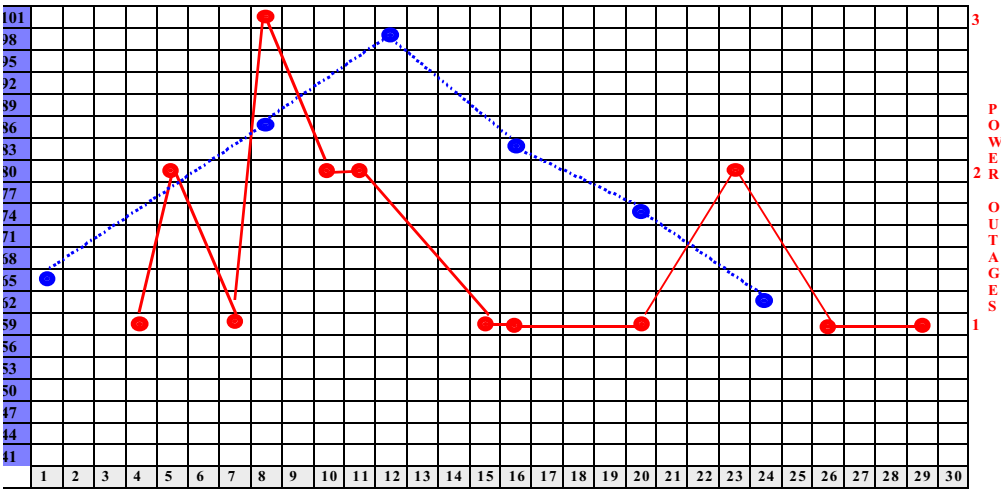

NOVEMBER 1999

Power Outages

Sunspot Index

THE NUMBER OF POWER OUTAGES AND SUNSPOT INDEX FOR FEBRUARY 1999

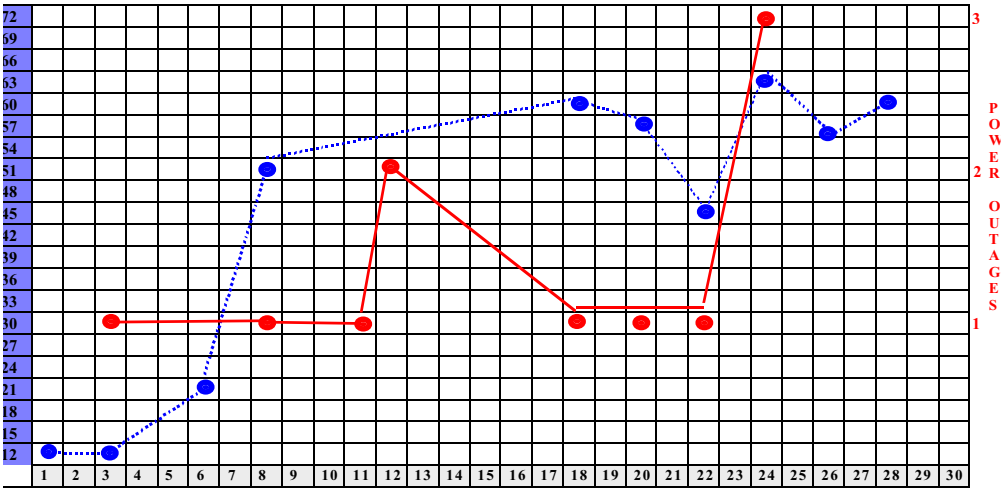

FEBRUARY 1999

Power Outages

Sunspot Index

THE NUMBER OF POWER OUTAGES AND SUNSPOT INDEX FOR FEBRUARY 1996

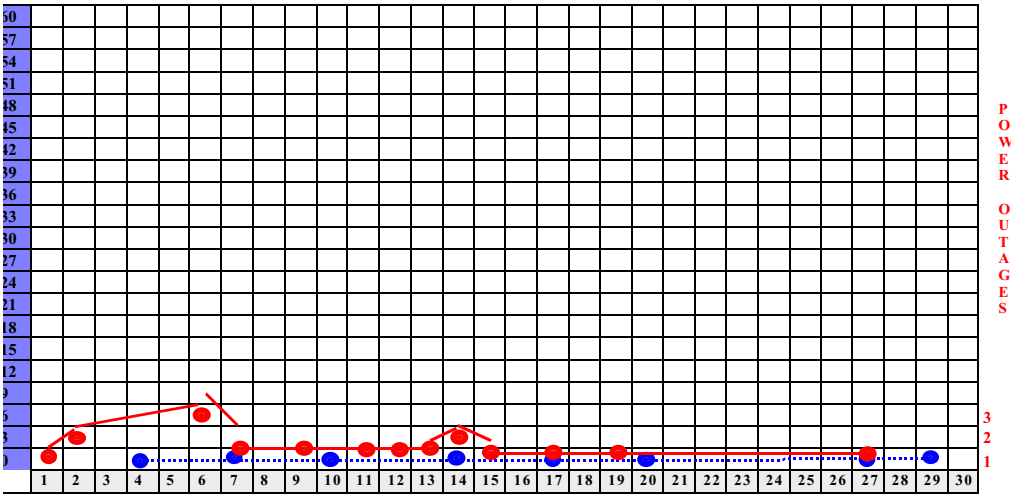

Power Outages

Sunspot Index

THE NUMBER OF POWER OUTAGES AND SUNSPOT INDEX FOR JULY 1996

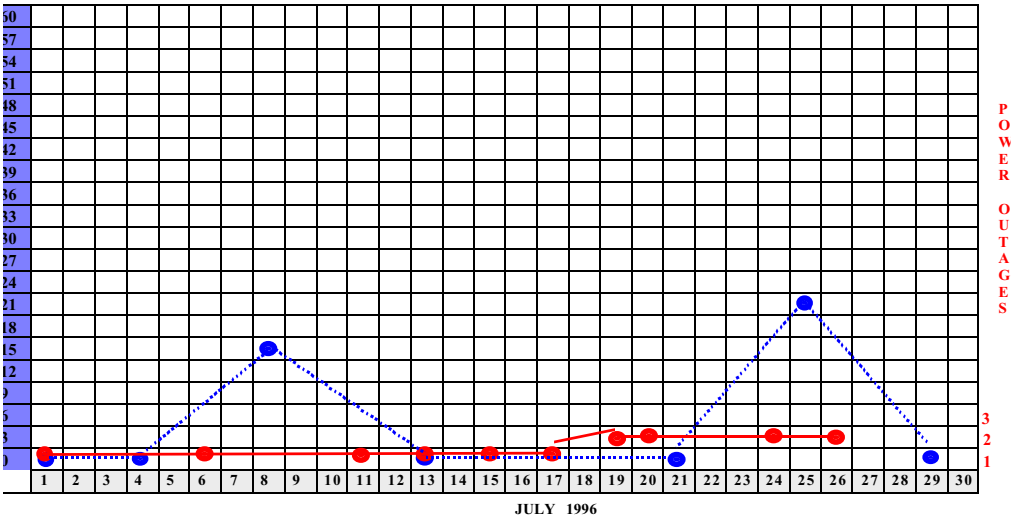

Power Outages

Sunspot Inde

THE NUMBER OF POWER OUTAGES AND SUNSPOT INDEX FOR NOVEMBER 1996

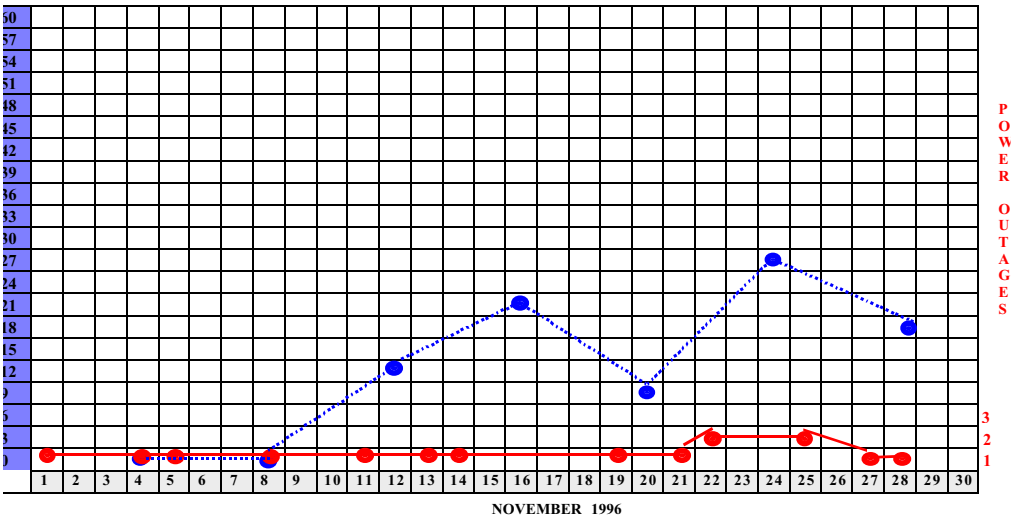

Power Outages

Sunspot Index

A Search for Novae in the Andromeda Galaxy - Year Two Results

Ken Phelps, Catherine Provenzano and the Nova Search 2000 Research Group
Grosse Pointe North High School, Grosse Point, MI
Teacher: Ardis Maciolek, RBSE '98

Abstract

The second year of this Nova Search project had two purposes: to follow up on four of the novae from last year's observations and to analyze two new sets of data. The four novae from last year were all seen in the last epoch (16) and it wasn't certain whether they would still be visible. Of the four epoch 16 novae, two continued to be seen in the new data fields. Light curves for those two were recalculated and their type was changed from NC to NB. Ten new novae were discovered. Of these, light curves for two could be calculated and they were found to be Type NB. The mosaics of nova types and nova locations were revised. The total of two years of class research has produced 31 novae with an average magnitude of 16.20 and a range of 15.23-17.69. Type NA novae, with fast decay light curves tend to be more centrally located in the galaxy.

Background and Purpose

The purpose of the Nova Search project was to follow up on four of the novae from last year's observations and also take two new sets of data (called epochs) from this last year and analyze both of them. Four novae last year were seen in the last epoch (16) and it wasn't certain whether they would still be visible. The idea of finding novae is to see if there is any pattern to where in a galaxy they occur and if there is a pattern to what types are found and how they are distributed.

New Procedures

The Nova Research Team set some new procedures this year. Some previously discovered novae have been hard to find again. To locate novae on the images more easily a new scale column was created in the data table. It lists the scale values used to see the novae. Another new data column was added to all new observations this year: standard stars. These are the numbers of designated comparison stars used to determine the magnitude of a nova.

Data Tables, Revised and New

The Data Tables contain many terms. Looking across from left to right it reads; nova, subraster, epoch, UT (universal time), right ascension, declination, magnitude, and scale. The column labeled "nova" lists that nova's assigned number. The subraster is the area of the galaxy where the nova was seen. The Andromeda Galaxy image is cut into sixteen of these for easier observation. The epoch is the day that each image was taken. Universal Time is equal to the time in Greenwich (the zero degree line of longitude- the prime meridian). The reason that the observation is done in UT (universal time) is so people observing from all areas of the world can have a standard time for easier comparing between observers. The x and y are the image coordinates of the nova.

There are two sets of data tables. The first set is the Nova Data 1999 table, containing Novae 1-21. It will not be published here, due to space constraints. This year some improvements were made in magnitude revisions, and some minor errors were corrected. The scale column was added.

The Nova Data 2000 table lists Novae 20 and 21 again, this time with new observations added from this year's research. Novae 22 –32 are new discoveries from this year.

Analysis

The standard stars already had a predetermined magnitude and a range of error, determined by NOAO. After using NIH Image to calculate the magnitude of the nova, the computer was asked to recalculate the magnitude of the comparison stars. The number it came up with was subtracted from the real magnitude on the standard star charts. Thus, an image error was produced. Then the error of the standard star charts (standard star error) was combined with the image error of the nova magnitudes, and using the square root of the sum of their squares divided by 2, a combined

error was reached.

The light curve graphs were made with magnitude on the Y- axis, and the time between the images were taken, was on the X-axis. If the nova only appeared on one image, it had no X value, so it couldn't be plotted, and in turn, couldn't be determined what type it was. The numbers of the magnitudes were made negative to ensure the graph went in the correct direction, which was decreasing. Error bars were made using the largest combined error for each nova. Three different types of curve fits, suggested by the NOAO, were tried. Included in these were a first, second, and third order polynomial. Since a nova can't go up and down in magnitude more than once in the time frame that was examined, the objective here was to get a curve that only showed one cycle. The R^2 value in the curve fit options, was the determining factor in which graphs to use. The closer the value is to 1.000, the better the fit. So, if two graphs both looked acceptable, which ever had a closer R^2 to 1.000 was the one that was chosen.

At this point, the type of nova was determined as NA, NB, or NC. Then, for every nova found, its position was plotted on the subraster maps. Next, all the dots from the new novae that were on the separate subraster maps were transferred onto the main map, which was a composite of the Andromeda Galaxy. These maps will be available for inspection on the astronomy class web page at:

http://north.gp.k12.mi.us/~maciola/webpages/

Four new light curve graphs were made. All four were determined to be type NB novae. Combining two years of data, the average magnitude of the novae was 16.20 and they ranged from 17.69 to 15.23. They are shown on the next page.

Conclusions and Extensions

Two of the four novae seen in epoch 16 were found again and new magnitudes and light curves were calculated for them. Based on the new analyses, they were changed from what they had been previously classified (Type NC) to Type NB. Ten new novae have been discovered. Two of the ten had multiple observations, so light curves were plotted for them. They were both classified as Type NB.

By examining the locations of the novae, there is no obvious reason why they are distributed this way, other than to conclude that where there are more stars, there are likely to be more novae. However, when looking at the type distribution, all the fast (NA) novae tended to be located nearer the center.

Light Curves of Novae - Year 2000

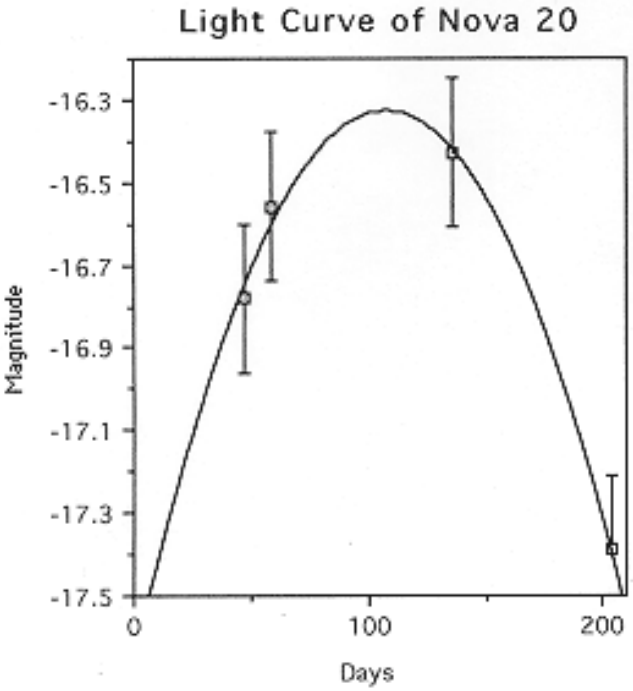

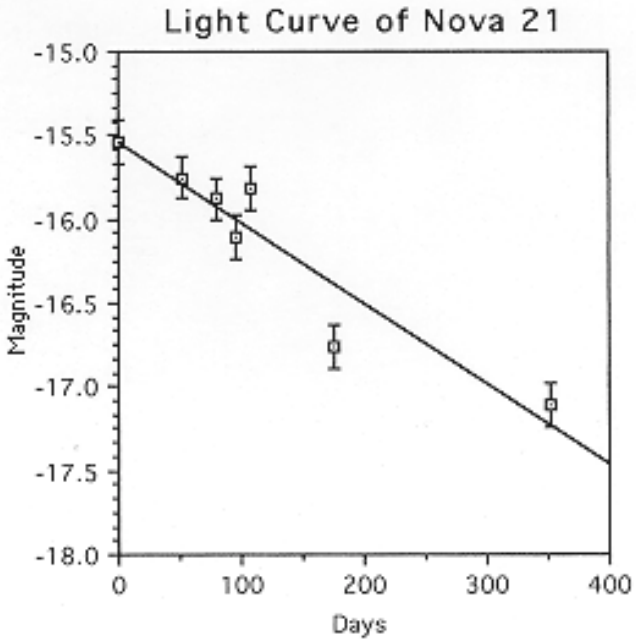

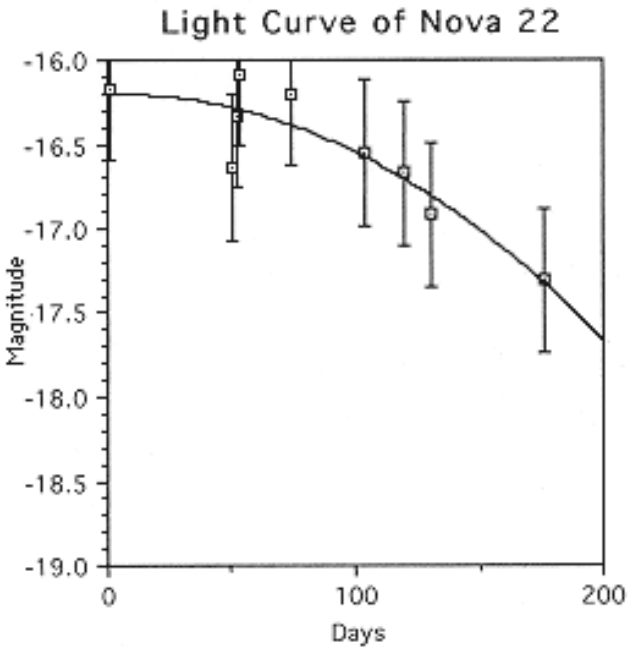

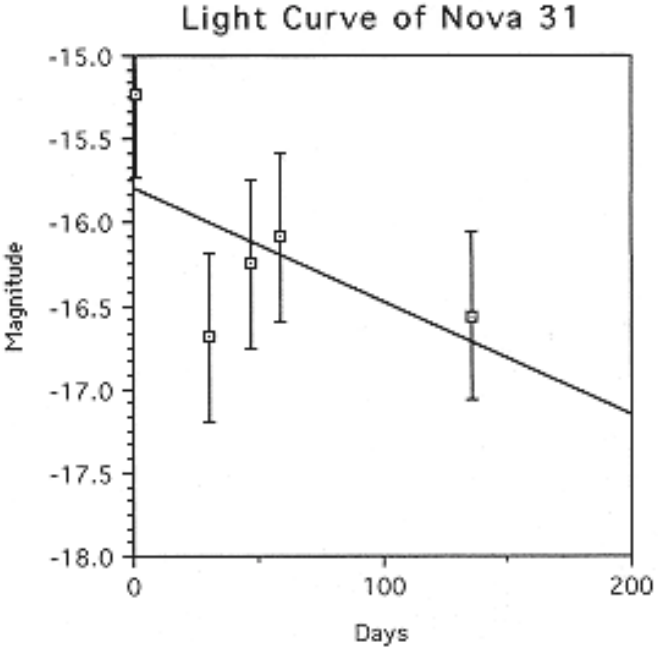

NOVA ANALYSIS CHART 2000

Nova	Image Error	Standard Stars	S.S. Error	Combined Error	Fit Method	Fit Correlation	Nova Type
20	0.02	95, 97, 103	0.09	0.07	P2	0.995	NB
20	0.24	95, 97, 103	0.09	0.18	P2	0.995	NB
20	0.06	95, 97, 103	0.09	0.08	P2	0.995	NB
20	0.00	95, 97, 103	0.09	0.06	P2	0.995	NB
21	0.15	107, 110	0.10	0.13	P1	0.853	NB
21	0.15	107, 110	0.10	0.13	P1	0.853	NB
21	0.15	107, 110	0.10	0.13	P1	0.853	NB
21	0.15	107, 110	0.10	0.13	P1	0.853	NB
21	0.15	107, 110	0.10	0.13	P1	0.853	NB
21	0.15	107, 110	0.10	0.13	P1	0.853	NB
21	0.15	107, 110	0.10	0.13	P1	0.853	NB
22	0.00	10, 12, 17	0.06	0.04	P1	0.424	NB
22	0.06	10, 12, 17	0.06	0.06	P1	0.424	NB
22	0.60	10, 12, 17	0.06	0.43	P1	0.424	NB
22	0.09	10, 12, 17	0.06	0.08	P1	0.424	NB
22	0.15	10, 12, 17	0.06	0.11	P1	0.424	NB
22	0.29	10, 12, 17	0.06	0.21	P1	0.424	NB
22	0.40	10, 12, 17	0.06	0.29	P1	0.424	NB
22	0.28	10, 12, 17	0.06	0.20	P1	0.424	NB
22	0.30	10, 12, 17	0.06	0.22	P1	0.424	NB
23	0.01	10, 12, 17	0.06	0.04			
24	0.04	22, 23, 24	0.06	0.05			
25	0.03	24, 18, 19	0.06	0.05			
26	0.18	84, 89, 91	0.08	0.14			
27	0.12	63, 72, 73, 74	0.11	0.12			
28	0.12	72, 73, 74	0.06	0.09			
29	0.03	103, 97, 95	0.09	0.07			
30	0.15	95, 97, 103	0.09	0.12			
31	0.14	106, 108, 109	0.09	0.12	P1	0.354	NB
31	0.10	106, 108, 109	0.09	0.10	P1	0.354	NB
31	0.16	106, 108, 109	0.09	0.13	P1	0.354	NB
31	0.13	106, 108, 109	0.09	0.11	P1	0.354	NB
31	0.70	106, 108, 109	0.09	0.50	P1	0.354	NB

The Correlation of the Location of Novae in the Andromeda Galaxy with Respect to the Duration of their Light Curves

Matt Harriger
Harry A. Burke High School, Omaha, NE
Teacher: Tom Gehringer, RBSE '98

Abstract

Novae in M31, the Andromeda galaxy, were located in images received from the 0.9 meter telescope at Kitt Peak National Observatory. Novae were located using the "blinking" method. Magnitude readings were taken for each epoch that a nova appeared in and light curves were developed for each nova. The location of the novae within the galaxy was then studied to determine where the greatest concentration of novae occurred. The location of novae relative to the duration of their light curve was also studied.

Purpose

The question to be addressed in this research is whether novae in the central part of M31, the Andromeda galaxy, are distributed evenly throughout the area or are found in greater concentration in specific areas.

Procedure

Novae are located on images of the central portion of M31 provided by the National Optical Astronomy Observatory through the Use of Astronomy in research-Based Science Education program. Images are provided on CD-ROM. Images were taken on 18 nights over a period of about three years. The NIH Image program is used to stack the images chronologically and switch rapidly between the images. Any star which appears in one image and not in the previous image is considered to be a possible nova.

After verification, magnitude readings are taken for each nova using a macro for the NIH Image program. The macro uses the known magnitudes of several standard stars within an image as calibration, then reads the magnitude of the nova. Light curves for each nova are then developed showing magnitude of the nova over time.

The location of each nova is then plotted on a large image of M31 to allow study of the distribution of the novae. Novae are compared with their proximity to the core of the galaxy to determine where the greatest concentration of novae lies.

Controls and Error Analysis

Nova candidates were checked to ensure that they really were novae and not artifacts from the CCD chip used in capturing the image. The program was used to zoom in on possible novae to ensure that they had fuzzy edges as opposed to sharp rectangular edges. Sharp edges mean a CCD artifact.

Also, possible novae that appeared in only one epoch were not used because they are more likely to be something other than novae appearing in more than one image. Novae appearing in only one image were also of little use to the research.

Many of the light curves obtained had a shape that differed from the generally accepted shape for a nova light curve. This is most likely due to the large gaps of time between some images. In those gaps it is not known what the magnitude of the nova is, leading to the strange light curves.

The sporadic nature of the images also leads to some error in determining the actual duration of the nova, as the point at which it fades out of view is not known exactly, but only to the date of the last epoch the nova appeared in. This error must be accepted in this research, as there is no way to eliminate it using the available data.

Data

Table 1 lists the magnitudes of all novae in each epoch they were visible in. The X, Y pixel coordinate of each nova and the julian date of each epoch is also given.

Nova	Epoch	Magnitude	X	Y	Light Curve Graph
F5e2-7	2	17.50	362	39	Figure 1
F5e2-7	3	17.81	362	39	Figure 1
F5e2-7	4	17.80	362	39	Figure 1
F5e2-7	5	17.64	362	39	Figure 1
F5e2-7	6	17.71	362	39	Figure 1
F5e2-7	7	17.53	362	39	Figure 1
F5e10-16	10	16.68	276	36	Figure 2
F5e10-16	11	16.76	276	36	Figure 2
F5e10-16	12	16.26	276	36	Figure 2
F5e10-16	13	16.52	276	36	Figure 2
F5e10-16	14	17.02	276	36	Figure 2
F5e10-16	15	17.25	276	36	Figure 2
F5e10-16	16	17.26	276	36	Figure 2
F6e10-17	10	15.67	131	340	Figure 3
F6e10-17	11	15.70	131	340	Figure 3
F6e10-17	12	15.84	131	340	Figure 3
F6e10-17	13	16.02	131	340	Figure 3
F6e10-17	14	16.47	131	340	Figure 3
F6e10-17	15	16.55	131	340	Figure 3
F6e10-17	16	16.86	131	340	Figure 3
F6e10-17	17	17.05	131	340	Figure 3
F6e14-17	14	16.49	378	493	Figure 4
F6e14-17	15	16.48	378	493	Figure 4
F6e14-17	16	16.41	378	493	Figure 4
F6e14-17	17	16.27	378	493	Figure 4
F7e3-8	3	15.87	412	489	Figure 5
F7e3-8	4	15.85	412	489	Figure 5
F7e3-8	5	15.76	412	489	Figure 5
F7e3-8	6	16.04	412	489	Figure 5
F7e3-8	7	16.06	412	489	Figure 5
F7e3-8	8	17.89	412	489	Figure 5
F7e10-13	10	15.81	117	438	Figure 6
F7e10-13	11	15.66	117	438	Figure 6
F7e10-13	12	16.51	117	438	Figure 6
F7e10-13	13	16.70	117	438	Figure 6
F7e10-15	10	16.34	228	467	Figure 7
F7e10-15	11	15.51	228	467	Figure 7
F7e10-15	12	18.15	228	467	Figure 7
F7e10-15	13	18.42	228	467	Figure 7
F7e10-15	15	18.3	228	467	Figure 7
F7e10-15	15	18.65	228	467	Figure 7
F10e3-7	3	16.12	194	12	Figure 8
F10e3-7	4	16.14	194	12	Figure 8
F10e3-7	5	16.06	194	12	Figure 8
F10e3-7	6	16.26	194	12	Figure 8
F10e3-7	7	16.38	194	12	Figure 8
F11e2-7	2	15.75	69	30	Figure 9

Analysis

Light curves for each nova were developed using Microsoft Excel. These light curves are shown in figures 1 through 12. The magnitude values for each epoch and corresponding julian date were inserted in a table and the chart function of the program was used to make an X, Y scatter style graph. This type of graph simply connected the points with straight lines, giving a good indication of the general trend of the magnitude.

Duration of each nova was approximated by the difference between the julian date of the first epoch in which the nova appeared and the julian date of the last epoch in which the nova appeared. The locations of the novae were then plotted on an image of the galaxy, along with their durations. Visual inspection was used to determine whether or not a correlation existed between the location of nova and its duration.

Conclusions

Twelve novae were discovered in the Andromeda Galaxy. Their magnitudes were determined for each epoch they were visible in. Their durations were compared with their locations in the galaxy to determine if a correlation existed.

No correlation was found between location and duration of light curve. Novae at similar distances from the core had widely varying durations. However, those novae that were very distant from the core had the longest light curves.

Acknowledgements

I would like to thank Dr. Travis Rector for his development of the procedures used to locate the novae and determine their magnitude. I would also like to thank my teacher Tom Gehringer for all of his help in making this research possible.

References

Rector, Dr. Travis, RBSE Nova Search Information. National Optical Astronomy Observatories,1999.

Bizony, M. T. The Space Encyclopedia E.P. Dutton, New York, 1960

Shipman, Harry L. The Restless Universe Houghton Mifflin, 1978

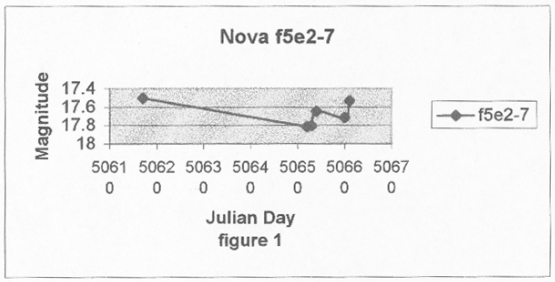

figure 1

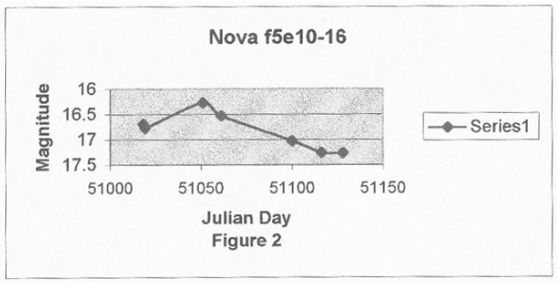

Figure 2

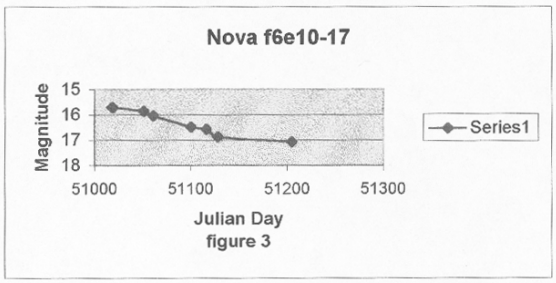

figure 3

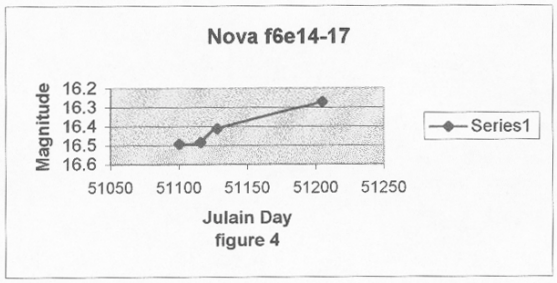

figure 4

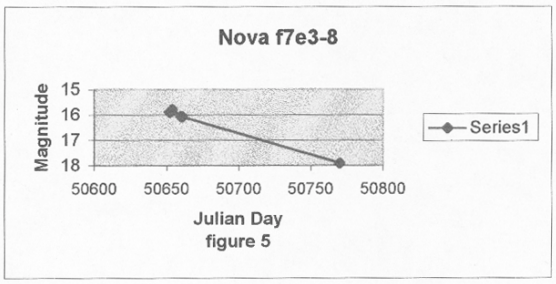

figure 5

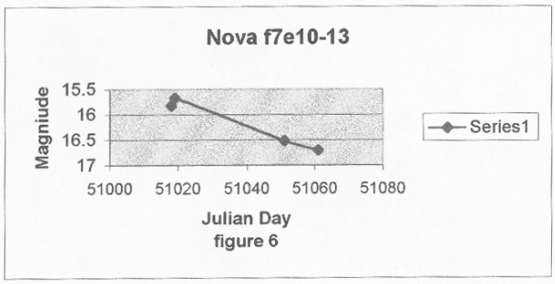

figure 6

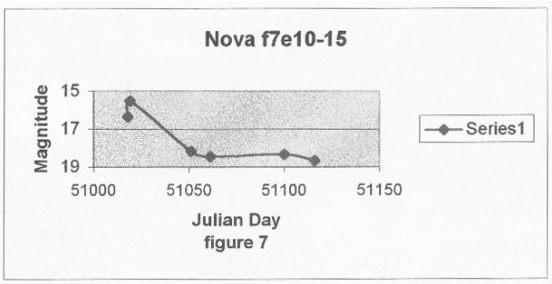

figure 7

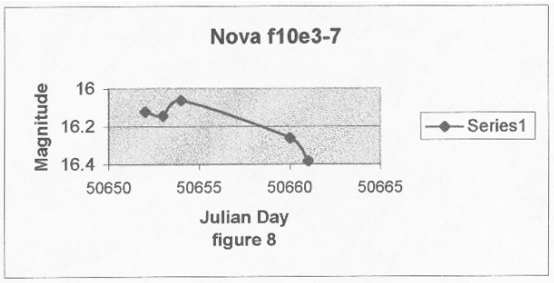

figure 8

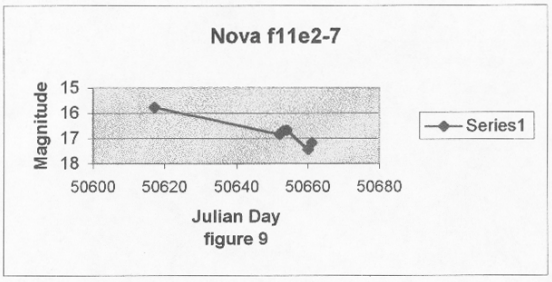

figure 9

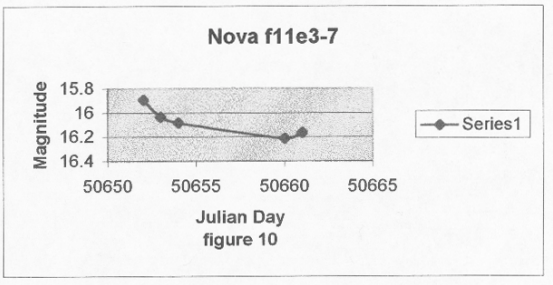

figure 10

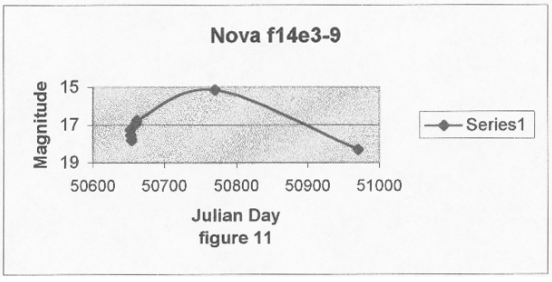

figure 11

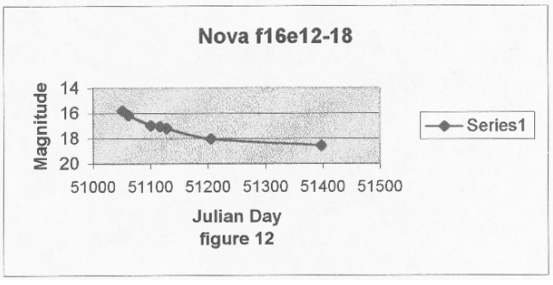

figure 12

The Search for Novae in the M31 Galaxy

Ben Nascenzi
Cranston East High School, Cranston, RI
Teacher: Howard Chun, RBSE '99

Abstract

55 possible novae were discovered in the Andromeda (M31) Galaxy. 18 data fields taken at Kitt Peak Observatory by a 0.9-meter telescope from 1995-1999 were scrutinized for stars that showed a sudden brightening or appeared from nowhere and disappeared a short time later.

Purpose

The purpose of this research project was to search for novae in the Andromeda Galaxy.

Procedure

The National Optical Astronomy Observatories supplied digital images on a RBSE CD-ROM. The CD contained images taken of M31 on 18 nights, irregularly spaced from September 1995 to July 1999. All pictures were ten-minute exposures through a Ha filter at 656.3nm.

The images were analyzed using software provided on the CD-ROM: Scion Image Beta 3 for the Windows 9x-based system. Special Macros written for this program allowed the importing of "*.FITS" files, the extension under which the images were saved.

The M31 galaxy was divided into 16 sections, or fields. Each field contained 18 files, one for each epoch. The times for the Epochs were as follows:

epoch 1	3-Sep-95
epoch 2	18-Jun-97
epoch 3	23-Jul-97
epoch 4	24-Jul-97
epoch 5	25-Jul-97
epoch 6	31-Jul-97
epoch 7	1-Aug-97
epoch 8	18-Nov-97
epoch 9	6-Jun-98
epoch 10	24-Jul-98
epoch 11	25-Jul-98
epoch 12	26-Aug-98
epoch 13	5-Sep-98
epoch 14	14-Oct-98
epoch 15	30-Oct-98
epoch 16	11-Nov-98
epoch 17	27-Jan-99
epoch 18	20-Jul-99

Using the Scion Image program, the first of the 18 epochs of each field was imported. Then, using the "rescale" command, the x,y values of the image were modified to a minimum value of 75, and maximum values of 200-1250, where the highest y values were set to view the area in the center of the galaxy (Fields 6, 7, 10, 11), and the lower y values were set to view novae on the outer skirts of the galaxy. Once the rest of the epochs were imported under the proper scale, a "stack" was created. This created a single slideshow of all the images.

The Stack was then animated to search for the novae. Novae were identified by stars that would "blink" into and out of existence, or current stars that would fade into nothing.

The Ha filter removes all but one wavelength of light used for observing. The novae emit the majority of their light at this wavelength, therefore making them easier to detect by using this filter.

Once all the possible novae for this field were identified, its location was recorded by determining their "x,y" pixel coordinates.

Control and Error Analysis

There were several scenarios that eliminated false nova possibilities. One of the factors was the edges of the picture. On some epochs the edges of the data was corrupted. No data could be taken in these areas. Another way of eliminating false novae is by zooming in on the object. When magnified, square or rectangular shapes indicate bad/false novae.

To verify authenticity, each field was examined three times, each using a different scale. This was used to verify the existing novae and to search for new ones. This was done to accurately verify the found novae, and to make this experiment repeatable.

Many of the novae found appeared for only one image only. Due to the sporadic dates the images were taken, it is possible that these are novae.

Due to technical problems inherent within the actual program, values for magnitudes and Right Ascention and Declination could not be calculated, thus making it difficult to compare these results with results found by Garavaglia, et al.

Data

Field #	# of Novae	(X, Y)	Epoch Dates
1	1	453, 59	10-11
2	0		
3	2	338, 116; 423, 510	1-10; 2-8
4	0		
5	4	277, 37; 167, 129; 362, 38; 458, 97	9-18; 17-18; 2-9; 8-14
6	13	34, 20; 171, 213; 132, 340; 112, 473; 126, 449; 134, 358;	2-9;17-18; 9-18; 1-2; 16-17; 9-11;
		376, 494; 416, 454; 451, 444; 510, 424; 481, 425; 466, 327; 468, 402	12-18; 14-17; 11; 11; 11; 11; 11
7	6	104, 90; 412, 490; 412, 488; 230, 467; 117, 437; 6, 447	14-17; 3-9; 3-8; 10-14; 10-12; 1
8	2	188, 186; 29, 377	1; 17
9	2	456, 236; 373, 48	11-12; 11-12
10	8	221, 48; 165, 107; 194, 12; 290, 145; 480, 440; 476, 115; 423, 93; 496, 56	18; 7-8; 3-8; 11; 1; 13-10; 18; 11
11	9	16, 405; 374, 397; 410, 165; 380, 331; 257, 218; 69, 30; 204, 121; 38, 82; 97, 158	16; 14-18; 2-10; 8; 31; 2-7; 3-8; 8; 18
12	3	434, 21; 392, 402; 43, 237	1-17; 2-8; 2-6
13	1	476, 190	5-12
14	1	426, 226	3-17
15	1	193, 470	13-18
16	2	15, 214; 95, 170	12-18; 2-8

Analysis and Conclusion

Fifty-five novae were located and verified in the entire range of images. Field six contained the most amount of novae, having 13 identified novae. The next highest amount of novae were discovered in fields 10 and 11. These fields were located toward the center of the galaxy. Refer to the chart below. As taken from the data discovered, it is apparent that novae tend to form closest to the center of a galaxy. In comparison to the search conducted by Garavaglia, et al, 49 more novae were discovered. That search, however, contained novae which were not discovered in this search.

References

A Search for Novae in the Andromeda Galaxy, Garavaglia, Jeff, et al. 1999 RBSE Journal

A Search for Novae in the Bulge of M31, Rector, T.A., et al. RBSE Nova Search Team, National Optical Astronomy Observatories. 2000

The Correlation of Active Galactic Nucleus Type with Distance as Determined by the Redshift of Spectral Signatures

Ryan Westerlin
Harry A. Burke High School, Omaha, NE
Teacher: Tom Gehringer, RBSE '98

Abstract

Spectroscopy is a key tool in the study of astronomy. Determining distances of objects is crucial because it informs astronomers of the possible origins and evolution of the universe. Active Galactic Nuclei are the main objects studied in the project. These objects include elliptical galaxies, starburst galaxies, radio galaxies, BL Lac objects, and quasars. My research asks the question, "Is their any correlation between distance to the object and its type?" My hypothesis is that, indeed, these objects exist at different distances. To prove this, I first had to classify each object according to its spectrum. Once each object was classified, their redshift, an indication of distance, was calculated. After determining the redshift, the actual distances to the objects were found by applying Hubble's Law. There appears to be a correlation between the type of object and its distance from Earth. Due to the finite speed of light, objects at greater distances are further in the past. The findings may indicate an evolution of galaxies.

Purpose

The purpose of this research project was to identify different objects according to their type, then determine their redshift and distance.

Procedure

Most of the spectra were obtained with the 2.1-meter telescope at Kitt Peak National Observatory, located about 40 miles west of Tucson, Arizona. Additional spectra were also obtained with the 3-meter telescope at Lick Observatory and the 3.5-meter telescope at Apache Point Observatory. The spectra cover the entire optical spectrum (what we can see with our eyes) as well as parts of the ultraviolet and infrared. These spectra were provided by the National Optical Astronomy Observatories on a CD-ROM as part of *The Use of Astronomy in Research Based Science Education* program.

The objects identified are from the FIRST survey and are given the prefix "FFS". The FIRST survey (which is an acronym for "Faint Images of the Radio Sky at Twenty-centimeters") is a radio survey of a portion of the night sky with the Very Large Array (VLA) radio telescope in New Mexico. Assembled by Dr. Sally Laurent-Muehleisen at the Lawrence Livermore National Laboratory, this catalog contains objects which emit radio waves. These spectra were obtained by Dr. Laurent-Muehleisen to identify these newly discovered radio sources. Because they emit radio waves, elliptical galaxies, starburst galaxies, quasars, BL Lac objects and other types of AGN are numerous.

Spectroscopy is a key tool in the development of my research. Spectroscopy is the study of "what kinds" of light we see from an object. It is a measure of the quantity of each color of light (or more specifically, the amount of each wavelength of light). In fact, most of what we know in astronomy is due to spectroscopy. Spectroscopy is done at all wavelengths of the electromagnetic spectrum, from radio waves to gamma rays; but optical light is what I used.

Not only are spectra used to determine an object's identity, but also its distance. Spectroscopy is used to determine an object's velocity towards or away from us via the *Doppler effect*. The Doppler effect on light is similar to that of sound. As an object emitting light moves towards you, the wavelengths become shorter (i.e., they become bluer; the light is said to be *blueshifted*). Conversely, if the object is moving away from you, the wavelengths of emitted light become longer (i.e., the light is *redshifted*). This shift is readily noticeable in the emission or absorption lines in an object's spectrum. The amount of shift is given by the following equation:

$$z = (\lambda obs/\lambda rest) - 1$$

In the above equation, "lobs " is the observed wavelength of an emission or absorption line (i.e., what you measure from the spectrum), lrest " is the "rest" wavelength of a line (i.e., what you would measure if the object were not moving) and "z" is the *redshift* of the object. It is important to note that a redshifted spectrum is not only shifted but is also stretched. The separation between any two lines therefore increases with redshift. However, the ratio of the wavelengths of the two lines does *not* change; that is, if you take the ratio of the above equation for two lines *at the same redshift* (e.g., lines "A" and "B"), the (1+z) redshift term cancels out, giving:

$$\lambda \text{ A obs} / \lambda \text{ B obs} = \lambda \text{ A rest} / \lambda \text{ B rest}$$

The objects' observed wavelengths are found by using the Graphical Analysis program by Vernier Software. The two strongest emission lines are determined, then, by utilizing the examine button on the program, the exact data point is recorded. Next, the ratio of these two objects is calculated and it is then compared to an emission line ratio chart:

Emission Line Ratios

	Ly α	C IV	[C III]	Mg II	Hβ	[O III]	Hα
Ly α							
C IV	1.28						
C III]	1.57	1.23					
Mg II	2.31	1.81	1.47				
Hβ	4.01	3.14	2.55	1.74			
[O III]	4.13	3.23	2.62	1.79	1.03		
Hα	5.41	4.24	3.44	2.35	1.35	1.31	

Once the ratio was found, I determined what two elements were present based on the following chart:

Ly α	1213
C IV	1549
[C III]	1909
Mg II	2796,2803
Hβ	4861
[O III]	4959,5007
Hα	6563

After using the redshift formula, the final redshift could be determined by using actual rest wavelengths versus observed wavelengths. From the derived redshift, the velocity of the objects could be determined using the following equation:

$$v = cz(1+ 0.5z)/(1+z)$$

where "c" is the speed of light (3.0×10^5 km s^{-1}). The distance can then be determined by Hubble's Law:

$$d = v / H_0$$

where "d" is distance in Megaparsecs and H_0 is Hubble's constant of 75 km s^{-1}. Conclusions were drawn from the distances of the objects studied.

Controls and Error Analysis

There are certain factors that must be considered when analyzing the data. One factor that may give a false distance is the Hubble's constant used. I used 75 km s^{-1} while some astronomers use anywhere from 50-100 km s^{-1} . This would give a false distance in my charts.

Another possible room for error deals with the earth's atmosphere and other galaxies. It is possible that some absorption lines are false because the earth's atmosphere is distorting the readings. It is also possible that while looking at an object's spectroscopy, the emission and absorption lines are off because another galaxy is interfering.

The final possible error that could occur is solving the mathematical equations correctly. One little error in determining the distance or redshift of an object can provide false information. This is countered by placing the object on the redshift chart. If it follows the pattern as the other objects, then the data is most likely correct.

Data

These are the following data points that I have used to conduct my research. There are many more data points on the RBSE CD-ROM not used in my research. The one offset data point is the farthest object known in our universe from NASA.

Object	Redshift	Distance (light years)
Quasars		
Q FFS 0859+3802	0.305	3,391,550,578
Q FFS 1723+5236	2.525	11,097,446,115
Q FFS 1054+2703	1.402	9,187,485,141
Q FFS 0301+0118	1.225	8,657,267,094
BL Lac Object		
B FFS 0758+2705	0.11	1,355,935,666
B FFS 1052+4241	0.15	1,810,721,206
B FFS 1412+2978	0.12	1,471,511,710
B FFS 1707+3975	0.16	1,921,309,686
Radio Galaxy		
R FFS 0040+0125	0.23	2,661,552,788
R FFS 0742+2622	0.17	2,030,670,775
R FFS 0148+0019	0.092	1,144,707,763
R FFS 1718+4278	0.188	2,224,454,810
Elliptical Galaxy		
E FFS 0934+2413	0.07	880,924,985
E FFS 1534+2513	0.05	635,719,382
E FFS 1317+4115	0.08	1,001,595,273
E FFS 1325+3955	0.09	1,120,983,502
Starburst Galaxy		
S FFS 2341+0018	0.305	3,391,550,578

Analysis

There were 50 AGN objects verified according to their type and 17 verified according to their distance and redshift. The quasars had the highest redshift and distance out of the five different types of objects. The redshift of these objects ranged from 0.305-2.525. Their distance was also calculated. The distance of the closest quasar to earth was 3.3 billion light years and the one farthest away was 11 billion light years.

The radio galaxies came next in descending order. Object FFS 0148+0019 had a redshift of 0.092 and a distance of 1.14 billion light years. Object FFS 0040+0125 contained a redshift of 0.23 and a distance 2.7 billion light years. The one starburst galaxy discovered was object FFS 2341+0018, had a redshift of 0.305, and a distance of 3.4 billion light years.

The fourth type of object analyzed was a bl lac object. The redshift on the four objects was relatively similar, having redshifts ranging from only 0.11-0.16. The distances were also close together. The distances averaged about 1.6 billion light years for the bl lac objects.

The final type of AGN was an elliptical galaxy. This object was the found to be the closest to earth. The redshift was only an average of 0.07. The farthest distance was also only 1.1 billion light years, the closest object 0.63 billion light years.

Conclusions

After determining the redshift and corresponding distances to the different types of objects, a definite correlation was found to exist between active galactic nucleus type and distance. Quasars were found to be most distant followed by radio galaxies, starburst galaxies, BL Lac objects, and elliptical galaxies. The accompanying graph indicates the relationship between distance and object type.

This relationship could indicate an evolution of galaxies over time. A quasar is the most active of these object types and it is thought that it is the result of massive amounts of material being pulled into a supermassive black hole at the center of a young galaxy. As the supply of material dwindles, the power of the quasar lessens.

Further study could include an increase in the number of objects studied to determine if the correlation of object type with distance is indeed true. It is possible that what the results show is coincidence due to the limited number of objects studied. Other surveys of deep sky objects could be analyzed.

Acknowledgments

I would like to thank Mr. Tom Gehringer, my Astronomy instructor, and Dr. Travis A. Rector, National Optical Astronomy Observatories, Tucson, AZ USA.

References

Baade, Walter. Evolution of Stars & Galaxies. Harvard University Press: Cambridge, Massachusetts, 1963.

Berry, Adrian. The Iron Sun: Crossing the Universe Through Black Holes. E.P. Dutton: New York, New York, 1977.

Bondi, Hermann. Cosmology Now. Taplinger Publishing Company: New York, New York, 1973.

Rector, Travis. AGN Spectroscopy: Studying Natures Most Powerful "Monsters". RBSE Journal: Tucson, Arizona, 1999.

Sullivan, Walter. Black Holes: The Edge of Space, The End of Time. Anchor Press/ Doubleday: Garden City, New York, 1979.

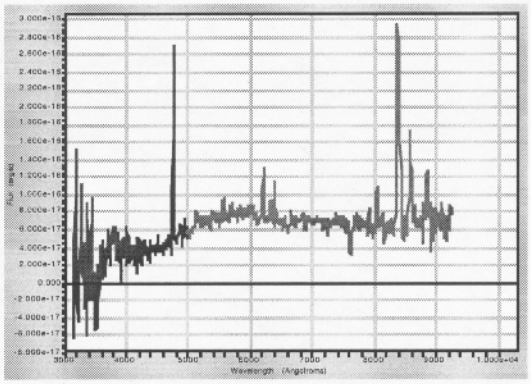

Typical Starburst Galaxy Spectrum

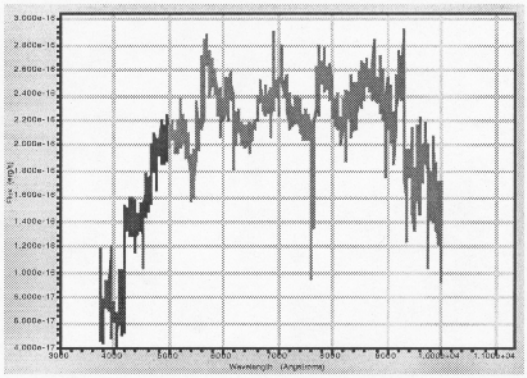

Typical Elliptical Galaxy Spectrum

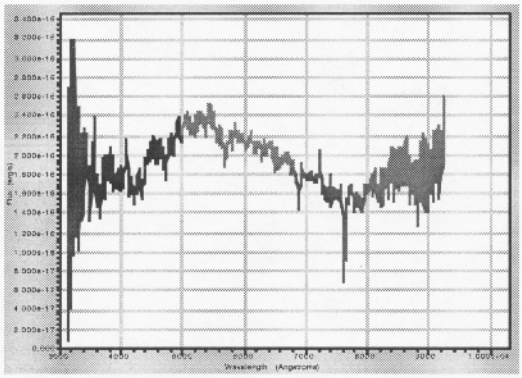

Typical Bl Lac Object Spectrum

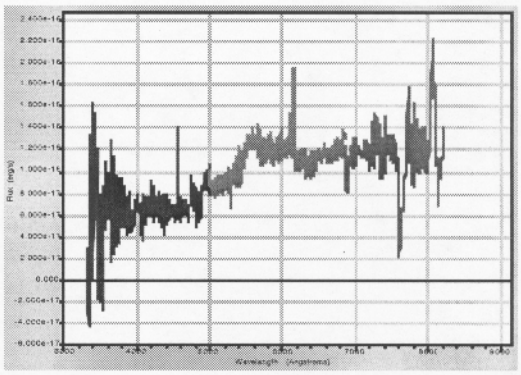

Typical Radio Galaxy Spectrum

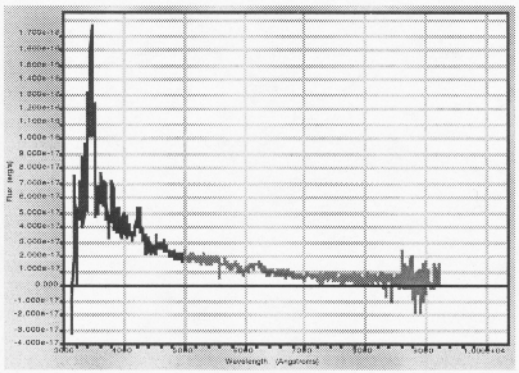

Typical Quasar Spectrum

Figure 1

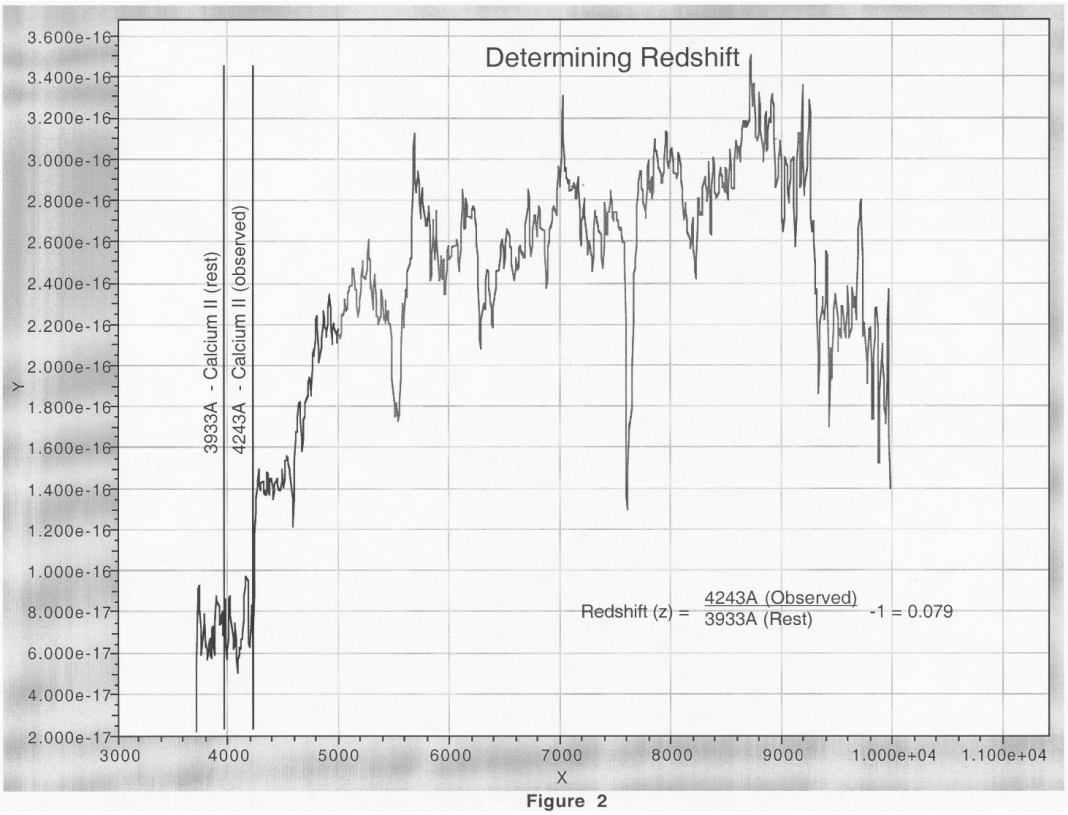

Figure 2

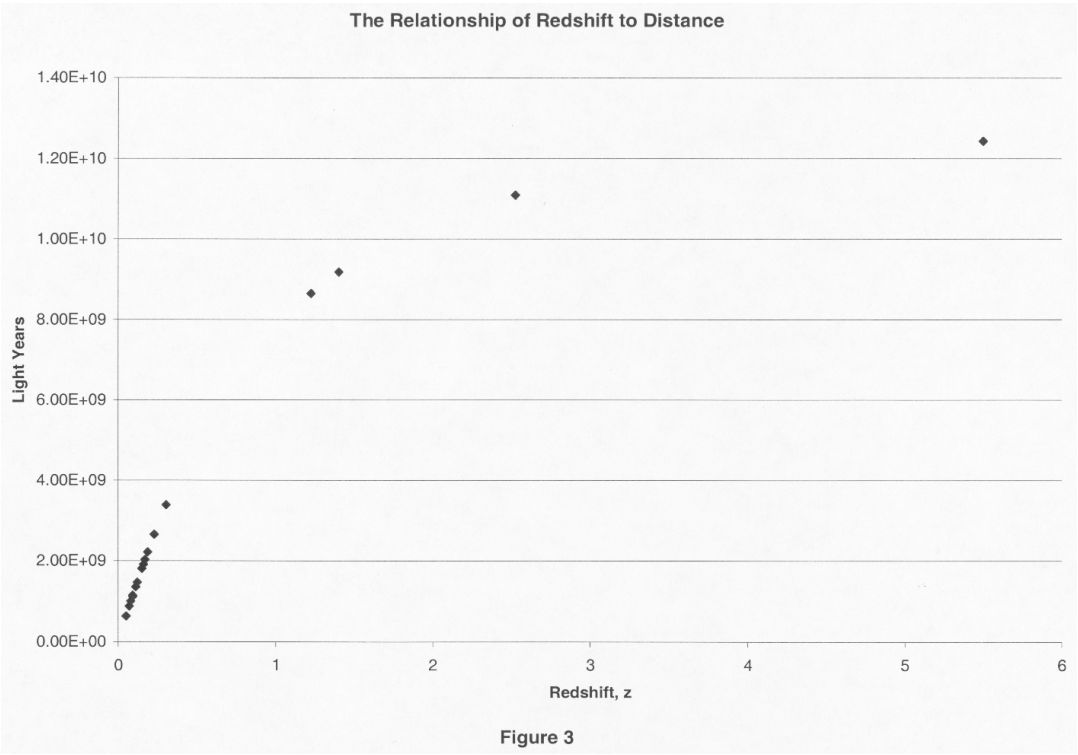

Figure 3

Investigating and Categorizing AGN Objects

Karyn Beaudry, Stephanie McClain, Ryan McCusker and Ethan Robinson
Cranston East High School, Cranston, RI
Teacher: Howard Chun, RBSE '99

Abstract

130 Active Galactic Nucleus objects (AGNs) in the Faint Images of the Radio Sky at Twenty cm (FIRST) survey were studied. 80 were determined to be quasars, 8 to be BL Lacs, 4 to be radio, 10 to be elliptical, and 10 to be starburst, in addition to 8 possible new category and 10 undefined objects. The data studied was in the form of spectral profiles, featuring the emission lines of the objects. The data was then examined to determine several things: the relationship of distance and luminosity of quasars, whether this luminosity was constant, whether there is any evolutionary progression of the objects, and classifying the possible new category objects. There appears to be a quadratic relationship between redshift and luminosity: the greater the redshift, the greater the luminosity, and therefore the younger the quasar. Luminosity for quasars was not constant. All objects other than quasars were scattered between redshift values of 0 and 0.3 with no clustering of the particular types, which seems to indicate that there is no evolutionary sequence among these types of galactic objects.

Purpose

The purpose of this project was to classify the 130 objects in this portion of the FIRST survey, and to discover any new relationships among them.

Procedure

Using the Graphic Analysis program, the researchers studied the spectral profile (which includes the continuous spectrum and emission and absorption lines; see fig. 1 through 5) of AGN objects in the FIRST survey, scattered in the sky over 10,000 square degrees of the North Galactic Cap (White 1997). The profiles were examined to determine values for redshift, calcium break, and the ratio of H_ to O_{III}, as well as to decide whether emission lines were narrow, broad, weak, strong, or not present. The emission lines are studied using the "full width, half max" (FWHM) method.

"FWHM is the width of the emission line at the halfway point between the base of the line (i.e., at the level of the continuum) and the peak of the emission line. In some cases the base of the emission line can be difficult to estimate because the continuum is not flat. While somewhat arbitrary, lines that have FWHM greater than 25 Å are considered to be broad, while lines with FWHM less than 25 Å are narrow." (Rector 22) To find the wavelength of the emission, the average of the two FWHM values is taken, resulting in the value for the center of the emission line.

Redshift is found by comparing the FWHM of two of the object's emission lines. After the values are obtained, the larger is divided by the smaller. The resulting number is compared to known ratios of non-redshifted emission lines. If the numbers are close, one divides the redshifted values by the non-redshifted values of these lines. The number obtained, minus one, is the redshift value.

The calcium break is a feature of most kinds of active galactic nuclei objects. The flux continuum rises dramatically around the CaII wavelength. Before this "break" there is a very noticeable doublet of absorption lines, which is the CaII absorption line pair. Because these are absorption lines, they could have been produced anywhere between the object and the observer, perhaps by an intermediate dust cloud. Because of this the redshift values obtained by analyzing them cannot be trusted to be the true values, but they can be taken as a minimum possible values. To measure the calcium break, one determines an average flux level before and an average one after the break and finds the percentage change (subtract the smaller from the larger and divide by the larger).

After finding fairly reliable data for all of these, one can attempt to determine what kind of object (out of elliptical, starburst, radio, quasar, and BL Lac) one is examining. Elliptical galaxies (fig. 1) have a calcium break usually

between 40% and 50%, are fairly nearby with redshifts of less than 0.1, and have no strong emission lines. Starburst galaxies (fig. 4) have calcium breaks less than about 40%, strong but narrow emission lines, and can be somewhat more distant, with redshifts less than 0.5, and have a H_{β} to O_{III} ratio of about 1. Radio galaxies (fig. 2) have all of the same characteristics as starburst except that the emission lines are not necessarily as strong and the H/O ratio is much less than 1. Quasars (fig. 3) are immediately recognizable as they have no calcium break and broad emission lines, and also have high redshift values (higher, usually much higher, than 0.5). BL Lacs (fig. 5) have no emission lines, calcium breaks less than 40%, and can have any redshift.

Controls and Error Analysis

There are several potential sources of error. The major one is that the data cannot be entirely trusted. Many factors, from sensor noise to intervening dust clouds, can cause the data to be inaccurate. Also, the emission lines are somewhat subjective: where one person sees one, another may see noise, and no number can be treated as being exact. To reduce error, the redshift number was used to find several valid emission lines in one object; if other confirming wavelengths were not found, the number was considered suspect. The FWHM method was also used to reduce error, as was the "statistics" function in the Graphic Analysis program, which produced a number for the average value of a certain area of the data, for use in calculating the calcium break. Some objects (such as BL Lacs) have no strong emission lines, which creates a problem in finding redshift; in these cases weak emission lines were used, but it is difficult to distinguish these from noise.

Data

See attachments.

Analysis

After the objects were identified as accurately as possible, and then classified as one of the five different radio emissions objects, comparison of the data was made concerning the relation of various trends identified within the data and within the five classification groups. Two projects analyzed the relation between redshift (age) and luminosity, using the equations $d=[cz(1+0.5z)/H_o(1+z)]$ to find distance, $v/c=((z+1)^2-1)/((z+1)^2+1)$ to find velocity, and $L=4\pi fd^2(1+z)^2$ to find Luminosity using distance, redshift, and flux. The flux was found by integrating between 4,000 and 8,000 Angstroms for each electromagnetic spectrum. The Hubble constant used (H_o) was 25 km/s / 1 million LY (Fraknoi 513). One project analyzed the data for possible evolutionary patterns; and the final project identified similar characteristics in 8 similar objects with myriad absorption lines.

The two projects that analyzed the luminosity of quasars and their possible relation to the redshift (age) identified a possible relationship between the two characteristics. It was identified that the younger quasars, with greater redshifts, had greater luminosity than the older quasars with smaller redshifts. Three curve fits were tried, linear, polynomial, and quadratic. The quadratic curve fit provided the smallest Mean Square Error, and displayed a noticeable underlying trend. Figures 8, 9, and 10 showed that the data points fall around the quadratic line curve approximation, with relatively few deviant points.

The project which attempted to identify if there was an evolutionary trend regarding the location and age of the 5 radio emissions groups identified that there was no noticeable grouping found among any of the 5 groups. Reference Figure 6 displays that each category of radio emissions objects do not cluster but are distributed evenly between 0 and 0.3 z. When interpreting the data of the five groups as a whole, Figure 8, a quadratic curve fit was also present.

The analysis of the characteristics of the non-quasar objects that remained of the original 120 AGN Objects showed that in eight particular objects the following trends were identified: the flux curve of each object took the form of a hill with a peak approximately at 9000 Angstroms, a large CaII break of approximately 47.05%, and an unshifted break of approximately 23.567% at 9300 Angstroms in each of the 8 objects. This break was not in the range of the telluric absorption bands and mirrored the characteristics of the CaII break.

References

Fraknoi, Andrew, David Morrison, Sidney Wolff, Voyages Through the Universe. Saunders College Publishing, 1997.

Rector, Travis, "AGN Spectroscopy." RBSE, 1999.

Data Table

Quasars

File	Redshift	E-Line Width	Ca II	V (km/s)	D (ly)
301	2.48	57	NONE	1.74E+05	6.97E+09
722	1.624	81	NONE	1.62E+05	6.50E+09
732	1.438		NONE	1.58E+05	6.32E+09
733	1.441		NONE	1.58E+05	6.32E+09
737	0.097		NONE	3.22E+04	1.29E+09
738b	3.060		NONE	1.78E+05	7.14E+09
740	0.712		NONE	1.25E+05	5.01E+09
738b	3.060		NONE	1.78E+05	7.14E+09
740	0.712		NONE	1.25E+05	5.01E+09
800	1.613		NONE	1.62E+05	6.49E+09
811	2.695		NONE	1.76E+05	7.04E+09
816	1.393		NONE	1.57E+05	6.27E+09
847	0.061		NONE	2.12E+04	8.49E+08
859	0.302		NONE	7.79E+04	3.12E+09
905	1.239	52	NONE	1.52E+05	6.08E+09
928	1.902	35	NONE	1.67E+05	6.70E+09
955	2.111	29	NONE	1.70E+05	6.81E+09
957	2.975	39	NONE	1.78E+05	7.12E+09
1001	3.7	19	NONE	1.81E+05	7.26E+09
1005	2.0	91	NONE	1.69E+05	6.76E+09
1006	3.67	77	NONE	1.81E+05	7.25E+09
1011	2.42	72	NONE	1.74E+05	6.95E+09
1019	1.75	80	NONE	1.65E+05	6.60E+09
1030	1.75	see 1019	NONE	1.65E+05	6.60E+09
1036a	3.64	43	NONE	1.81E+05	7.25E+09
1036b	2.01	86	NONE	1.69E+05	6.76E+09
1039	0.79		NONE	1.31E+05	5.23E+09
1047	0.03		NONE	1.09E+04	4.36E+08
1054	0.99		NONE	1.42E+05	5.68E+09
1106	0.15		NONE	4.63E+04	1.85E+09
1112	1.5		NONE	1.60E+05	6.38E+09
1119	1.53		NONE	1.60E+05	6.41E+09
1131	1.855		NONE	1.67E+05	6.67E+09
1143	2.6		NONE	1.75E+05	7.01E+09
1144	2.6		NONE	1.75E+05	7.01E+09
1152	0.48		NONE	1.03E+05	4.13E+09
1157	1.8		NONE	1.66E+05	6.63E+09
1210	1.95		NONE	1.68E+05	6.73E+09
1223	2.4		NONE	1.74E+05	6.94E+09
1238	2.4		NONE	1.74E+05	6.94E+09
1254	1.65		NONE	1.63E+05	6.52E+09
1257	1.5		NONE	1.60E+05	6.38E+09
1306	1.6		NONE	1.62E+05	6.48E+09
1318	0.05		NONE	1.77E+04	7.07E+08
1334a	1.35		NONE	1.56E+05	6.22E+09
1334b	0.18		NONE	5.35E+04	2.14E+09
1335	1.7		NONE	1.64E+05	6.56E+09
1349	1.2		NONE	1.51E+05	6.03E+09
1351	2.15		NONE	1.71E+05	6.83E+09
1359	1.83		NONE	1.66E+05	6.65E+09
1406	2.56		NONE	1.75E+05	7.00E+09
1408	0.846		NONE	1.34E+05	5.37E+09
1410	0.14		NONE	4.38E+04	1.75E+09
1430	0.22		NONE	6.23E+04	2.49E+09
1448	2.5		NONE	1.74E+05	6.98E+09
1450	0.71		NONE	1.25E+05	5.00E+09
1501	2.3		NONE	1.73E+05	6.90E+09
1517	0.137		NONE	4.30E+04	1.72E+09
1533	0.76		NONE	1.29E+05	5.15E+09
1534b	3.1		NONE	1.79E+05	7.15E+09
1534c	1.29		NONE	1.54E+05	6.15E+09
1535	2.14		NONE	1.71E+05	6.83E+09
1537	0.46		NONE	1.01E+05	4.03E+09
1545	1.77		NONE	1.65E+05	6.61E+09
1546	1.25		NONE	1.52E+05	6.10E+09
1557	3.7		NONE	1.81E+05	7.26E+09
1602	1.78		NONE	1.65E+05	6.62E+09
1606	1.76		NONE	1.65E+05	6.60E+09
1608	3.97		NONE	1.82E+05	7.29E+09
1614b	1.55		NONE	1.61E+05	6.43E+09
1616	2.26		NONE	1.72E+05	6.88E+09
1619	2.35		NONE	1.73E+05	6.92E+09
1620	2.1		NONE	1.70E+05	6.81E+09
1627	2.54		NONE	1.75E+05	6.99E+09
1628	2.25		NONE	1.72E+05	6.88E+09
1630	0.18		NONE	5.35E+04	2.14E+09
1639	0.87		NONE	1.36E+05	5.43E+09
1641	2.75		NONE	1.76E+05	7.06E+09
1656	0.65		NONE	1.20E+05	4.81E+09
1658	2.11		NONE	1.70E+05	6.81E+09
1706	3.38		NONE	1.80E+05	7.20E+09
1708	1.34		NONE	1.55E+05	6.21E+09
1723	2.52		NONE	1.75E+05	6.99E+09
1724	0.6		NONE	1.16E+05	4.63E+09
2341	0.7		NONE	1.24E+05	4.97E+09

New Category

File	Redshift	E-Line Width	Ca II	ID?	New Ca II	? Break	V (km/s)	D (ly)
1049	0.063	13	38%	New category	40.3%	23.8%	90375	3.615E+09
	1.953	25						
	1.524	25						
1240	0.00088	10	46%	New category	53.4%	19.9%	101230	4.049E+09
	0.0013	14						
1317	0.0655	13	46%	New category	45.7%	23.9%	100865	4.035E+09
		19						
1325	0.074	19	46%	New category	46.4%	24.6%	100498	4.020E+09
		19						
1411	0.076	15	38%	New category	37.3%	25.4%	90807	3.632E+09
1534a	0.305	31	50%	New category	46.7%	22.7%	105556	4.222E+09
1614a	0.065		47%	New category	41.2%	21.0%	102074	4.083E+09
1649	undefined	undefined	?	New category	66.0%	27.1%	undefined	undefined

BL Lacs

File	Redshift	E-Line Width	Ca II	ID?	V (km/s)	D (ly)	
202	0.21	33	37%	BL-Lac	6.02E+04	2.41E+09	
		19					
218a	0.175	22	39%	BL-Lac	5.24E+04	2.10E+09	
		15					
218b	1.65	15	42%	BL-Lac	1.63E+05	6.52E+09	noisy:
	there were	13					hard to
	multipule	22					read
	red shifts	15					
754	undefined	none	11%?	BL-Lac	undefined	undeifined	
758	0.476	14	19%	BL-Lac	1.03E+05	4.11E+09	
	there were	19		Has a few e-lines			
	multipule	43					
	red shifts	43					
1036c	0.13	19	36%	BL-Lac	4.12E+04	1.65E+09	
		19					
		62					

Radio

File	Redshift	E-Line Width	Ca II	ID?	V (km/s)	D (ly)
40	0.23		23%	Radio	6.44E+04	2.58E+09
742a	0.1715	19	40%	Radio	5.16E+04	2.06E+09
936	0.076	10	46%	SB/Radio	2.59E+04	1.04E+09

Normal

File	Redshift	E-Line Width	Ca II	ID?	V (km/s)	D (ly)
20	0.07		45%	Normal	2.40E+04	9.62E+08
701	0.5	24	48%	Normal	1.06E+05	4.22E+09
728	0.33	24	50%	Normal	8.26E+04	3.30E+09
934	0.05	13	55%	Normal	1.77E+04	7.07E+08
1412	0.1145	19	53%	Normal	3.70E+04	1.48E+09
1707	0.0769	14	51%	Normal	2.62E+04	1.05E+09

Starbursts

File	Redshift	E-Line Width	Ca II	ID?	V (km/s)	D (ly)
148	0.115	19	41%	Starburst	3.72E+04	1.49E+09
254	0.0665	24	22%	Starburst	2.30E+04	9.18E+08
715	0.36	14	44%	Starburst	8.73E+04	3.49E+09
	there were	10				
	multipule	24				
	red shifts	38				
731	0.248	14	15%	Starburst	6.80E+04	2.72E+09
738a	0.2155	19	25%	Starburst	6.14E+04	2.46E+09
904	0.11	14	35%	Starburst	3.58E+04	1.43E+09
	there were	24				
	multipule	24				
	red shifts	38				
1052	0.14	24	29%	Starburst	4.38E+04	1.75E+09
		53		Radio		
		24				
1615	3.54	43	47%	Starburst	1.81E+05	7.23E+09
	there were	29		Radio		
	multipule	19				
	red shifts	19				
1655	0.075	19	37%	Starburst	2.56E+04	1.02E+09
1718	0.187	19	33%	Starburst	5.51E+04	2.21E+09
1725	0.062	19	41%	Starburst	2.15E+04	8.61E+08
2148	0.203	15	32%	Starburst	5.87E+04	2.35E+09
2327	0.1	7	34%	Starburst	3.30E+04	1.32E+09
2346	0.078	14	47%	Starburst	2.65E+04	1.06E+09

Figures

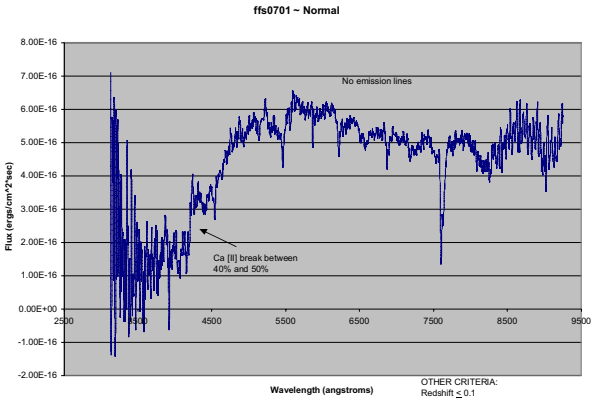

Figure 1

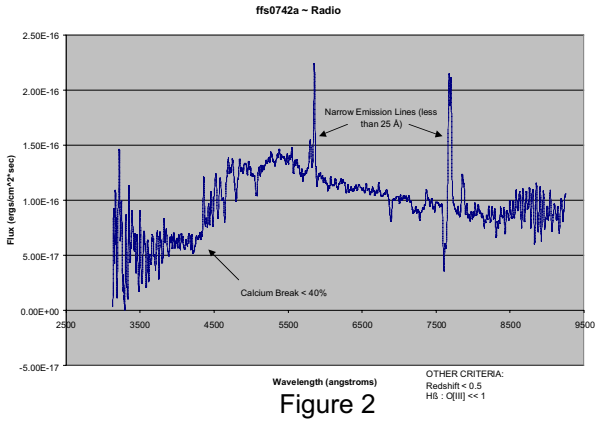

Figure 2

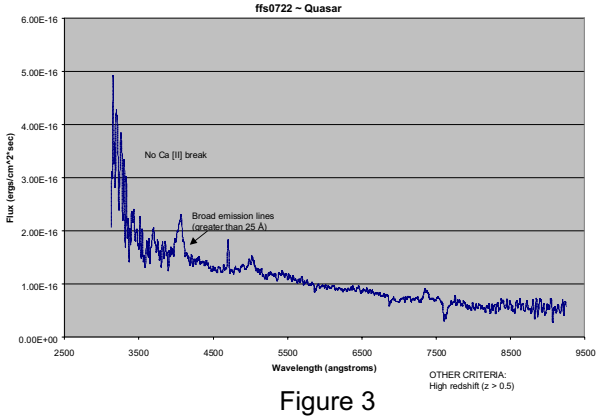

Figure 3

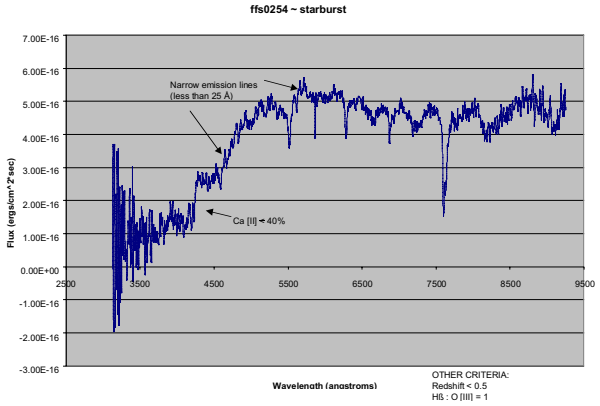

Figure 4

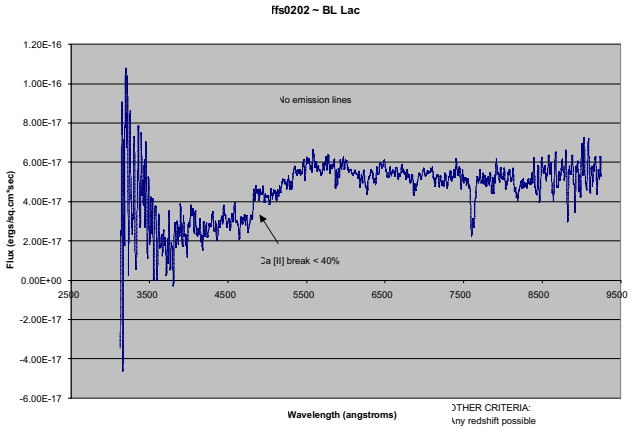

Figure 5

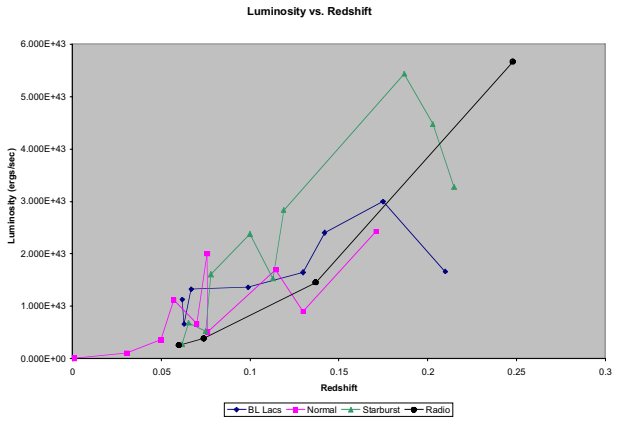

Figure 6

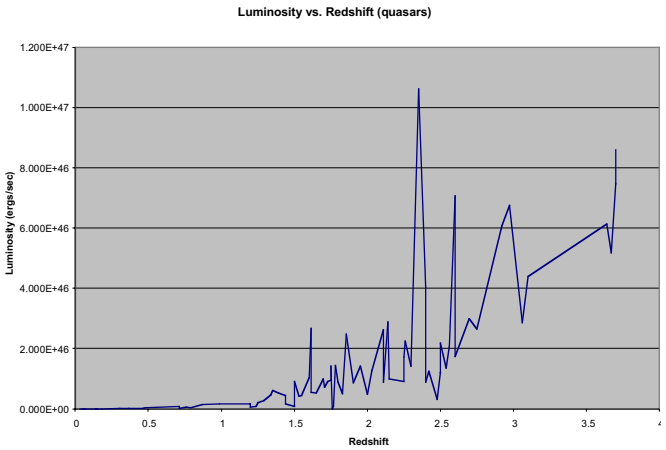

Figure 7

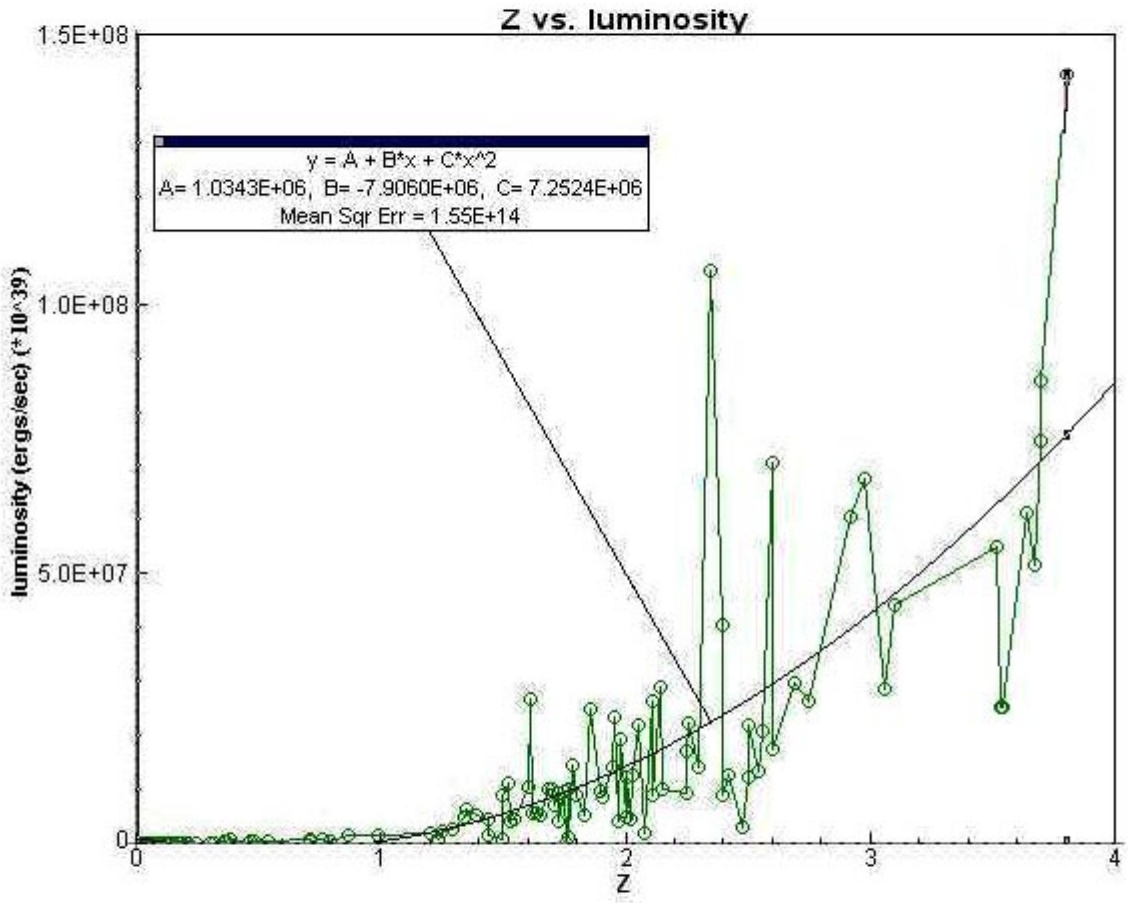
Z vs. luminosity
y = A + B*x + C*x^2
A= 1.0343E+06, B= -7.9060E+06, C= 7.2524E+06
Mean Sqr Err = 1.55E+14
luminosity (ergs/sec) (*10^39)
1.5E+08
1.0E+08
5.0E+07
0
0
1
2
3
4
Z

Figure 8

Figure 9: Quasars

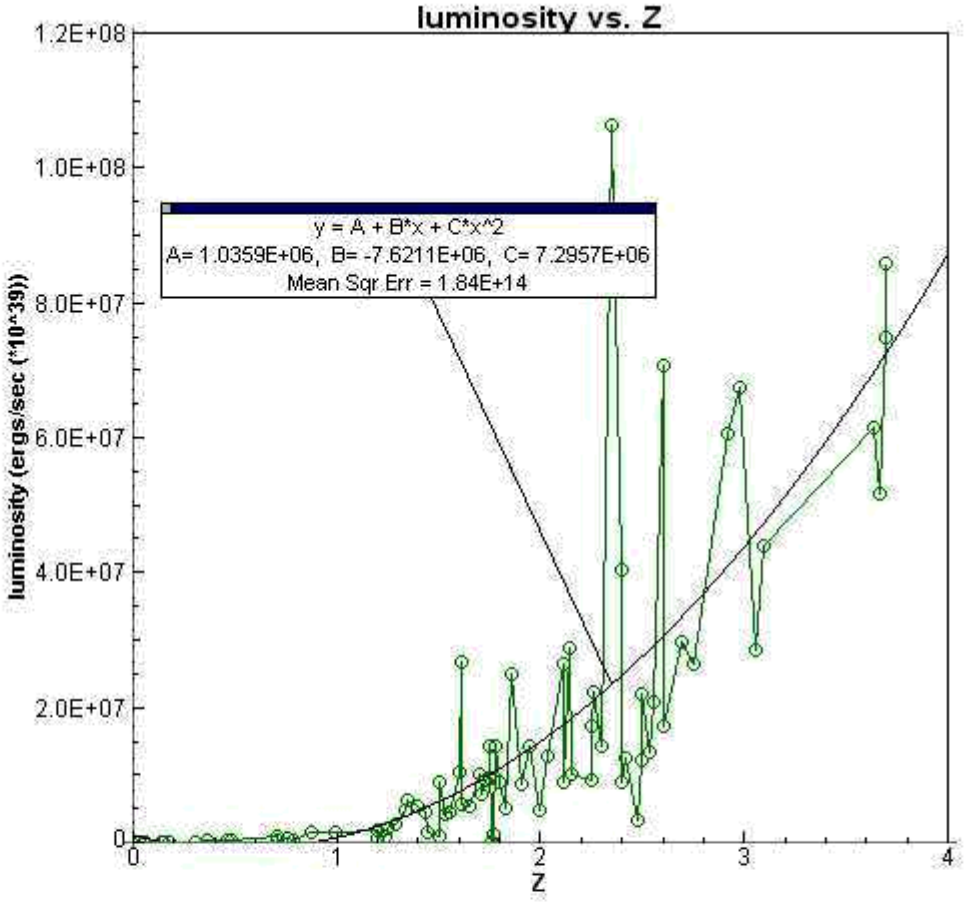

Figure 10: Other Categories